Late Holocene climate reconstructions for the Russian steppe, based on mineralogical and magnetic properties of buried palaeosols

T. Alekseeva [a], A. Alekseev [a,*], B.A. Maher [b], V. Demkin [a]

[a] Institute of Physicochemical and Biological Problems of Soil Science, Russian Academy of Sciences, Pushchino, Russia
[b] Centre for Environmental Magnetism and Palaeomagnetism, Lancaster Environment Centre,
Department of Geography, Lancaster University, Lancaster, LA1 4YB, UK

Abstract

Insights into past climate changes, and corresponding evolution of soils and the environment, can be gained by multi-disciplinary studies of palaeosols. Here, we focus on palaeosols buried beneath archaeological monuments, specifically, funerary mounds (kurgans), in the Russian steppe. The kurgans were constructed, and each of the palaeosols buried, over a range of different timesteps from the mid-Holocene to ∼ 600 years before present (yr BP). Integrated magnetic, mineralogical and pedological data were used to obtain estimates of past climate (especially precipitation) changes, through both time and space. A soil magnetism-based climofunction, derived previously from modern steppe soils and modern climate, was applied to each set of palaeosols, to obtain quantitative reconstructions of annual precipitation for the time at which the soils were buried. Independent soil property data (clay mineralogy, salt content, iron mineralogy from Mossbauer analysis, and optical and electron microscopy) were also obtained, in order to test and substantiate the magnetic inferences. The data obtained indicate that the climate of the Lower Volga steppe area has varied from the mid-Holocene onwards. Precipitation minima occurred at ∼ 5000, ∼ 3800, and ∼ 1600 yr BP, with intervals of enhanced precipitation at ∼ 1900 yr BP and ∼ 600 yr BP. These rainfall variations appear to occur synchronously with changes in Middle Eastern precipitation and lake levels, suggesting they are controlled by index changes in the North Atlantic Oscillation.

1. Introduction

Burial mounds (earth or stone hills), known in the Russian literature as 'kurgans', appeared across large areas of the Eurasian steppe from ∼ 5000 years ago. Funeral ceremonies with erection of such burial mounds occurred between 5000 and 600 yr BP. Until recently, the kurgans have been considered as objects of study for archaeology, ethnography, or other humanities; they provide key information about the culture of steppe inhabitants (Kimball et al., 2000) during the Bronze Age (III–II millennia BC, ∼ 5000–4000 yr BP), Early Iron Age (beginning I millennium BC–IV C. AD, ∼ 3000–1600 yr BP), and Middle Ages (V–XVI C. AD, ∼ 1500–500 yr BP). However, the kurgans also contain buried soils, which developed in past Holocene time-slices and have been preserved by burial up to the

* Corresponding author.
  E-mail address: aalekseev@rambler.ru (A. Alekseev).

present day. Palaeosols can act as integrative records of past climatic, lithological, geomorphological, geochemical, biological, and hydrological conditions (e.g. Wright, 1986; Retallack, 2001). The palaeosols buried by the very large number of kurgans (100s of thousands) on the Russian steppe can provide a database of quantitative and qualitative characteristics for environmental reconstruction at the moment of each kurgan's construction. The properties of these buried soils reflect, particularly, the climate, vegetation, and microrelief and thus can be used for reconstruction of palaeoenvironmental conditions. Because kurgans were constructed at different times from the mid-Holocene onwards, they preserve a range of palaeosols recording past environmental changes through this whole interval; indeed, kurgans of different ages are often sited close to each other, especially on watershed sites. Palaeosol properties sensitive to climatic and environmental change can include: the concentration and distributions of salts, carbonates, gypsum and humus; structures of their microbial communities; and stable isotope compositions of pedogenic carbonate and humus. So far for the kurgan palaeosols, qualitative changes in climate (especially humidity) have been inferred from carbonate content and distributions, assuming carbonate accumulation (B_{ca} horizon formation) during arid conditions and carbonate dispersion during relatively humid intervals (e.g. Demkin et al., 1998, 2004). On this basis, a period of desiccation has been inferred at $\sim$ 5000 years BP, reaching a maximum at $\sim$ 4000 BP, before wetter conditions prevailed at $\sim$ 3000 BP (e.g. Demkin and Ivanov, 1985; Demkin et al., 1989; Khokhlova et al., 2001, 2004). Recently, a quantitative, soil magnetism-based climofunction has been established for the area of the Russian steppe (Maher et al., 2002, 2003). For a set of 22 modern soils across the loessial plain of the Caucasus to the pre-Caspian region, the pedogenic magnetic susceptibility (magnetic susceptibility$_{B\ horizon}$ minus the magnetic susceptibility$_{C\ horizon}$) was found to be strongly correlated ($R^2 = 0.93$) with present day values of annual precipitation (Fig. 1). A similar correlation between rainfall and magnetic susceptibility was previously obtained for the Chinese Loess Plateau and explained as a result of pedogenic formation of magnetite and maghemite via oxidation/reduction processes through soil wetness events (Maher and Thompson, 1999).

Here, we examine the magnetic properties of a range of palaeosols of different ages, preserved beneath groups of kurgans constructed at five separate locations within the Russian steppe zone. We then apply the climofunction obtained from the steppe modern soils (Maher et al., 2002, 2003) to obtain, for the first time,

quantitative estimates of annual precipitation across this region at intervals through the last $\sim$ 5000 years. We also include quantitative magnetic extraction data to provide information on the pedogenic magnetic minerals (their mineralogy, composition, grain size, morphology) in palaeosols of different ages. Independent, rapidly developing (i.e. decades to centuries) soil properties studies include the humus content in the upper soil horizon, depth of easily soluble salts, gypsum and carbonate content, and the upper horizon magnetic properties. Clay mineralogy was also examined, since clay minerals are the main source of soil Fe (Schwertmann and Taylor, 1989; Alekseeva et al., 1989; Alekseev et al., 1996).

2. Materials and methods

The study area falls within the Lower Volga basin, which includes the Central Russian, Privolzhskaya, and Ergeni uplands and the Caspian Lowland, in the southern Russian Plain ($\sim$ 1200–1500 km south of Moscow, Fig. 1a and b). Modern climatic conditions across the Lower Volga basin are dry and warm, with mean annual precipitation of 350–400 mm and mean annual temperature of $\sim$ 11 °C. The modern climate reflects the continentality of the region, together with some rainshadow influence of the Caucasus range to the south/southwest. Precipitation, which is variably distributed through the year, arises in winter from frontal activity associated with penetration of moist Atlantic westerlies and in summer is mainly convectional. Many of the present day soils and the palaeosols are light (luvic) or dark (haplic) variants of kastanozem profiles (FAO/UNESCO classification), i.e. well-drained soils with brown, humic topsoils (Ah horizons, with >50% of roots concentrated in the upper 25 cm) overlying a brown/cinnamon, argic (clay-enriched) or cambic (slightly weathered) subsoil or B horizon with different degrees of solonetz features (i.e. often with carbonate and/or gypsum accumulation in or below the B horizon). The modern soil cover is characterized by a mosaic of kastanozems and solonetzes forming microcatenas, determined by surface microtopography. The solonetzes, which occupy about 40% of the territory (Demkin and Ivanov, 1985), are confined to flat micro-elevations whereas the light and dark kastanozems are associated with slopes and microdepressions, respectively.

Age control on the kurgans and their buried palaeosols has been gained previously from radiocarbon dating (AMS, e.g. Alekseev et al., 2002; Alexandrovskiy et al., 2001; LSC, e.g. Shishlina et al., 2000; Khokhlova et al., 2004) and archaeological artefacts.
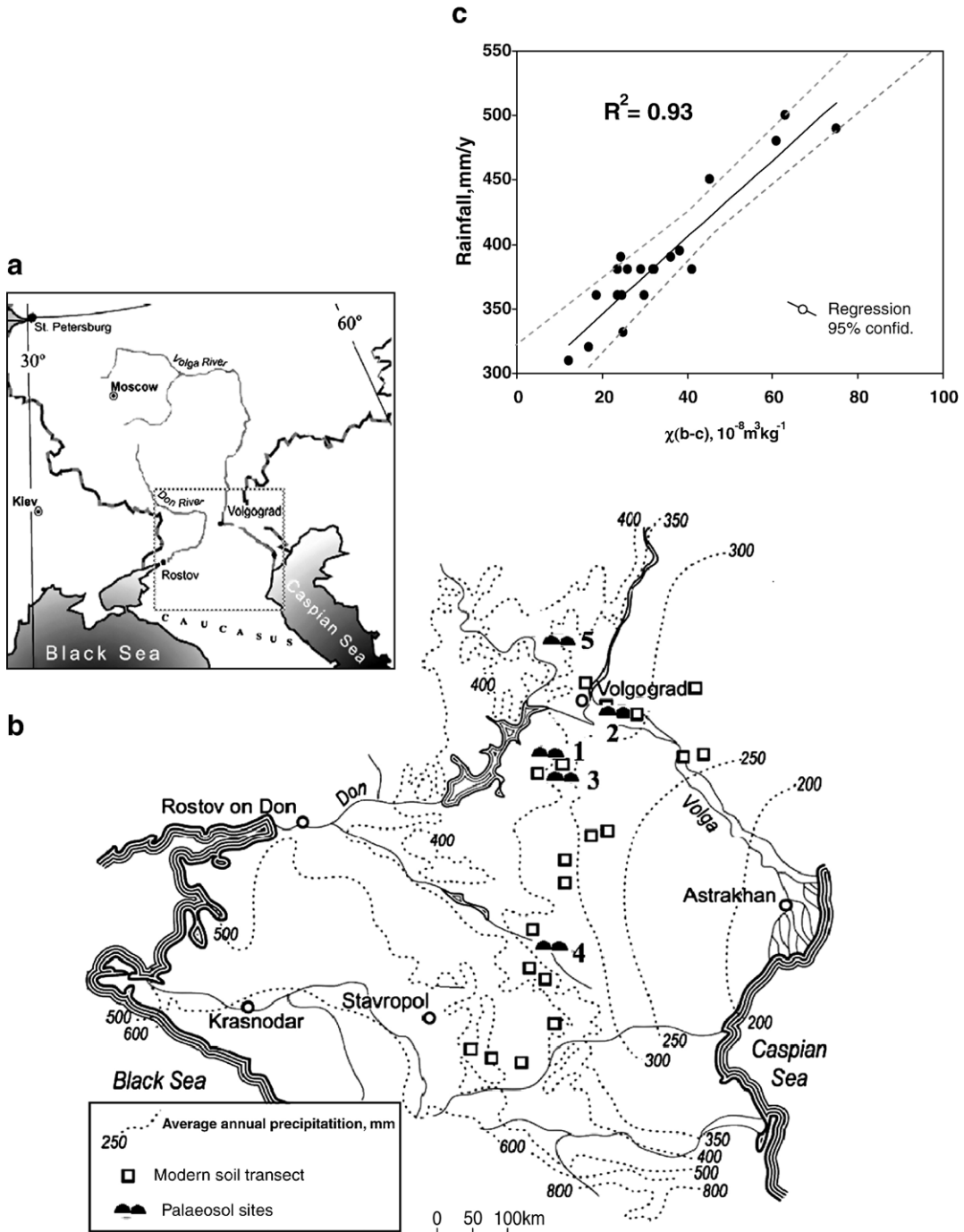
Fig. 1. a) Site location, including modern steppe soil transect of Maher et al. (2002, 2003); b) individual site location map with sample sites 1 – Abganerovo; 2 – Malyaevka; 3 – Peregruznoe; 4 – Kalmykia; 5 – Avilov; c) Pedogenic magnetic susceptibility versus annual precipitation for the Russian steppe, modern soil transect ($R^2 = 0.93$).

Table 1 summarises the relationship between distinctive archaeological cultures and an absolute, ^{14}C-based chronology. The distinctive cultures encapsulated within the kurgans (Skripkin, 1990; Sergatskov, 1994; Gelez-

chikov et al., 1995) provide the basis for age determination for particular burial mounds with an accuracy of e.g. ±100–200 yr for the Bronze Age to ±50 yr and less for the Middle Ages. Fig. 1a and b shows the

Table 1
Relationship between archaeological cultures in the Russian steppe and absolute (radiocarbon-determined) timescale, calendar yr BP

Archaeological epoch	Period	Time, yr BP	Radiocarbon dating
Present time Middle Ages	XX–XXI cent. AD	0–50	
	XV–XVII cent AD	300–500	
	XII–XIV cent. AD	600–800	625±25
			700±100
			700±100
			Khokhlova et al. (2004)
	V–IX cent. AD	900–1500	
Iron Age	Late Sarmatian (II–IV cent. AD)	1800–1600	1890±60 BP
			1825±25
			Khokhlova et al. (2004)
	Middle Sarmatian (I cent. BC– I cent. AD)	1900–2100	
	Early Sarmatian culture (400 BC–100 BC)	2100–2400	2320±50 Alekseev A.Y. et al. (2002)
			2250±50
			2325±25
			Khokhlova et al. (2004)
	Sauromatian culture (600 BC–400 BC)	2400–2600	2510±50
			2570±50 Alekseev A.Y. et al. (2002)
			2550±50 Khokhlova et al. (2004)
Bronze	Srubna or Timber-grave culture (2000 BC–1200 BC)	3200–4000–	3960±40 Shishlina et al. (2000)
	Catacomb culture (2700 BC–2000 BC)	4000–4700	4120±70
			4260±120
			4410±100 Shishlina et al. (2000)
			4400±100 Khokhlova et al. (2004)
	Yamna culture (III–II millennia BC)	4500–5200–	4900±100
			5200±100 Khokhlova et al. (2004)
Early Bronze Late Eneolithic	IV–III millennia BC	5000–6000	5100±50 Borisov et al. (2004)

location of the kurgans and sampled modern soils for the five investigated sites; Table 2 summarises the site locations, kurgan age information, parent materials and modern soil types present. As is often the case, several kurgans of different ages occur at each of the sites,

normally within an area of >1 km^2; for example, at Abganerovo, 30 kurgans of different ages are present (Fig. 2a and b). So far, at least 10 kurgans have been excavated at each of our investigated sites. Thus, a number of palaeosols have been preserved under differently aged kurgans at each site. These palaeosols represent the environment immediately prior to each episode of kurgan construction and soil burial within the past $\sim$ 5000 years (Fig. 2c and d). The palaeosols all have the same parent material and similar (watershed) topography, thus providing good control on the other soil-forming factors (Dokuchaev, 1883; Jenny, 1994) and effectively isolating soil variations due to climate and time.

All the palaeosol sequences were examined using a range of room temperature magnetic measurements (see Appendix 1 and e.g. Maher et al., 1999), including: low- and high-frequency magnetic susceptibility, anhysteretic remanence (ARM) and incremental acquisition of magnetic remanence (IRM) and af demagnetisation, and a high-field IRM (HIRM), af demagnetised in a field of 100 milliTesla (mT). For two selected sites (Abganerovo and Malyaevka), representative soil samples were also subjected to analysis of soil chemical properties and their clay mineralogy (by X-ray diffraction and Mössbauer spectroscopy). Magnetic extraction procedures were also used to concentrate the magnetic carriers for independent investigation by XRD and microscopy (optical and transmission electron microscopy). Prior to magnetic extraction, the samples were decalcified using buffered acetic acid and were then particle-sized into <38 and >38 µm fractions (Hounslow and Maher, 1996). Mineral grains were extracted using the magnetised probe method for the <38 µm fraction and the magnetic edge method for the >38 µm fraction (Hounslow and Maher, 1999). An additional, ultrafine ($<\sim$ 2 µm) magnetic separate was obtained by further magnetic concentration of the <38 µm magnetic extracts. The amount of magnetic material extracted at each stage was quantified by before- and after-extraction magnetic measurements (susceptibility, ARM). Mössbauer analysis (Appendix 2) was applied to representative bulk, clay fraction and magnetic extract (<38 µm) samples, and the relative contents of total and divalent iron, as well the proportions of magnetite (maghemite) and haematite, estimated from numerical analyses. The spectra were computer fitted with a number of overlapping Lorentzian peak lineshapes using a non-linear regression χ^2 minimization procedure. Clay fractions (<2 µm) from soils and parent material samples were separated by sedimentation after dispersion of samples in a wet paste. No additional chemical pre-treatments or ultrasonication were used for the dispersion. X-ray diffraction was used

Table 2
Summary of site locations, parent materials and modern soil types

Site name location	Latitude; longitude	Kurgan ages, ~ calendar yr BP	Modern soil types	Parent material
Abganerovo; Volgograd region	48°06′N, 43° 59′E	5000; 3800; 1700; 1600; 600	Light kastanozem and solonetzic	Calcareous, loess-like, silty clay loam
Peregruznoe; Volgograd region	47°45′N, 43°36′E	5800; 4500; 3800, 1900, 1800, 600	Light kastanozem and solonetzic soil	" "
Kalmykia; Zunda–Tolga, Mandzhikiny, Iki Burul district, Republic of Kalmykia	45°37′N; 44°25′E	5100±50; 4410±100; 4260±120; 4120±70; 3960±40; ~ 600	Kastanozem and solonetzic soil	" "
Malyaevka; Volgograd region	48°42′N, 45°28′E	~ 4500; ~ 3600; ~ 1700; ~ 600;	Light kastanozem and solonetzic soil	Silty clay deposits of marine origin
Avilov; Volgograd region	48°42′N, 45°28′E	~ 5100; ~ 4900; ~ 4000; ~ 1900; ~ 1750; ~ 700	Kastanozem and solonetzic soil	Calcareous, loess-like, silty clay loam

to identify their clay mineralogy (Appendix 2). Quantitative estimation of the main clay mineral groups was based on the Biscaye (1965) method.

3. Results

Table 3 summarises a range of soil properties for the five sets of palaeosol sequences and the modern soils.

All the soils are well-buffered, with pH values ranging from 7.0 to 9.6. Compared with the modern soils, the humus content in the A1 horizon of the buried soils is consistently less, indicating probable diagenetic loss of humus through time under burial (Gubin, 1984). With just a few exceptions (e.g. the Abganerovo and Avilov soils buried at ~ 600/700 yr BP), accumulation of calcium carbonate in the upper 50 cm of the modern soils
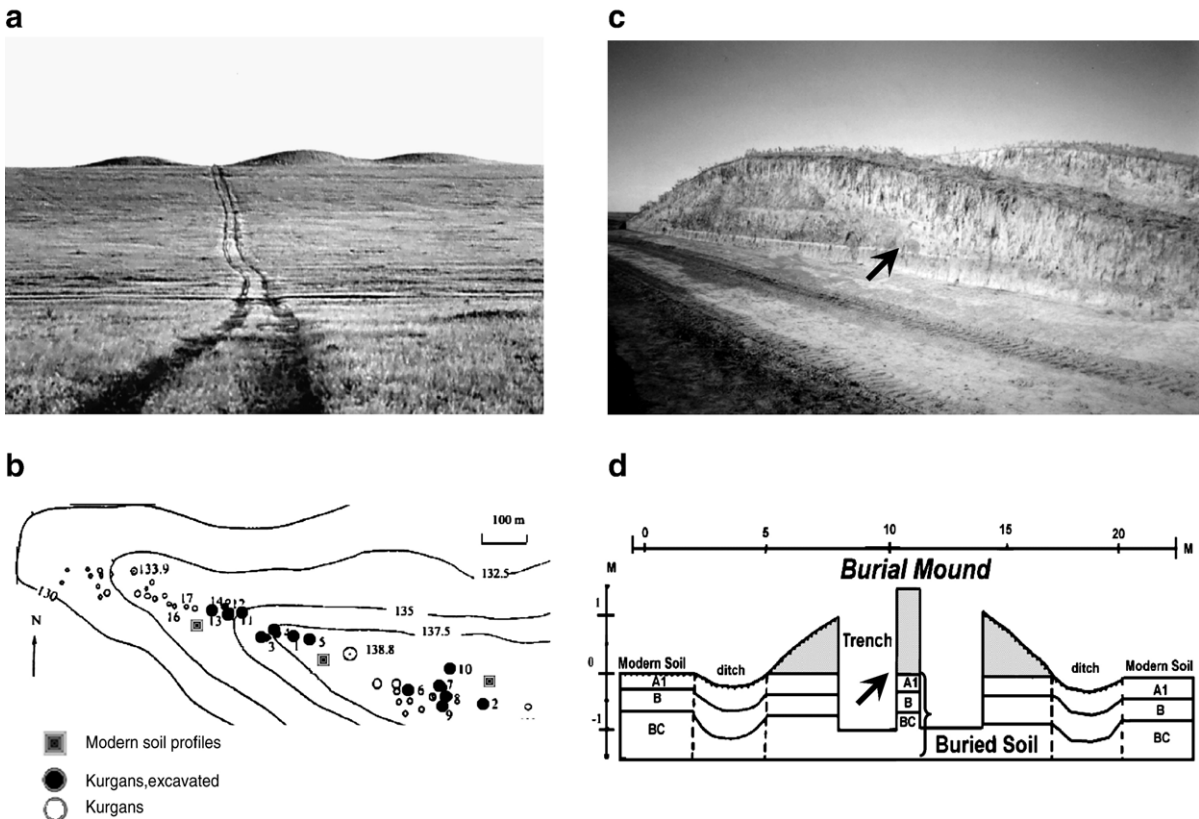

Fig. 2. a) Typical steppe environment with multiple kurgans of different ages located on the watershed; b) map of kurgan distribution at Abganerovo (with archaeologists' kurgan identifying local numbers near the excavated kurgans); c) section through an individual kurgan; d) schematic showing the location of a preserved palaeosol beneath the kurgan shown in photo c).

Table 3
Soil analytical data properties for the palaeosols and modern soils

Soil profile, age	Horizon	Depth, cm	Clay, %	Clay B/ clay A	Humus, %	pH	CaCO$_3$	Exchangeable cations (mg–eq/100 g)		
								Ca	Mg	Na
Malyaevka light kastanozem										
D-482, modern	A1	0–10	10	1.3	1.92	7.0	0.0	7.00	4.95	1.21
	B1	10–30	13		1.53	7.6	1.0	12.80	7.83	1.03
	B2	30–43	29		0.81	8.6	8.1	15.60	10.30	1.21
D-480, ~ 600 BP	A1	23–31	23	1.6	1.07	8.9	0.0	12.00	14.43	5.53
	B1	31–55	36		0.69	8.5	2.0	10.40	10.30	8.82
	B2	55–71	19		0.41	8.4	15.2	10.40	10.72	9.17
	C	135–155	11		–	8.5	8.2	–	–	–
D-476, ~ 1700 BP	A1	22–31	20	1.5	0.93	8.3	0.0	9.00	6.60	6.57
	B1	31–50	30		0.41	8.6	2.5	8.60	10.31	10.20
	C	78–150	18		–	8.3	7.5	–	–	–
D-481, ~ 3600 BP	A1	45–54	21	1.4	0.62	8.8	1.5	7.60	9.48	9.00
	B1	54–77	29		0.34	8.6	9.5	7.80	11.55	10.55
D-486, ~ 4500 BP	A1	68–76	27	0.9	0.83	7.0	1.8	9.20	7.90	6.40
	B1	76–105	24		0.50	8.0	2.4	10.80	9.16	6.92
	C	200–250	20		–	8.2	6.8	–	–	–
Solonetzes										
D-484, modern	A1	0–9	21	1.9	2.77	7.1	0.0	9.00	6.32	0.29
	B1	9–35	40		1.12	7.7	1.4	16.00	12.37	1.47
	B2	35–50	20		0.60	8.9	6.5	13.60	10.56	1.55
D-485, ~ 600 BP	A1	43–48	9	3.7	0.95	7.7	0.0	5.05	5.32	3.98
	B1	48–73	35		0.81	7.8	1.0	12.20	15.99	8.82
	B2	73–95	23		0.60	8.3	6.1	11.00	10.32	6.40
D-486	C	95–150	11		–	8.7	9.7	–	–	–
Abganerovo light kastanozem										
A99-5, modern	A1	0–10	19	1.1	2.53	8.1	0.0	14.10	7.65	1.03
	B1	10–20	21		2.24	8.2	0.0			
	B2	20–40	25		1.38	8.7	1.5	15.00	10.32	2.76
	C	105–200	13			9.0	8.6	9.05	8.99	6.22
D-414, ~ 600 BP	A1	47–57	21	1.0	1.37	7.0	0.0	15.80	7.32	0.86
	B1	57–72	21		1.30	7.2	0.0	20.09	3.80	0.33
	B2	72–87	19		1.19	7.5	0.0	25.21	8.02	0.47
	Bcca	87–102	12		–	8.0	8.0			
D-456, 1600 BP	A1	90–99	17	1.1	1.12	8.2	0.0	3.60	10.48	10.38
	B1	99–116	19		0.96	8.8	6.1	5.80	11.22	12.62
D-463, ~ 5000 BP	A1	104–114	13	1.4	0.36	8.8	0.0			
	B1	114–131	18		0.55	8.6	3.3	16.0	11.2	7.2
	C	250–400	13		–	9.0	8.4			
Solonetzes										
D-451, modern	A1	0–11	11	3.6	1.55	8.0	0.0	8.00	3.99	1.07
	B1	11–25	40		1.10	8.6	6.2	16.20	13.86	6.74
	Cg	120–200	25		–	8.3	10.8	7.00	10.98	8.13
D-455, ~ 1600 BP	A1	111–119	8	4.8	0.52	8.1	0.0	3.05	5.66	5.36
	B1	119–134	39		0.28	8.4	2.6	7.40	16.50	15.05
	C	351–371	21		–	8.7	10.3	4.05	9.99	14.18
	C	371–431	20		–	8.9	10.3			
D-464, ~ 3800 BP	A1	79–88	12	2.0	0.22	8.6	0.0	1.08	8.65	8.47
	B1	88–103	25		0.34	8.6	5.0	1.05	13.20	14.87
Kalmykia										
D-531, modern soil	A1	0–14	8	3.10	1.65	7.2	0.00	0.08	0.05	0.06
	B1	14–37	25		1.03	7.9	0.50	0.13	0.15	1.37
	C	95–180	15		–	8.4	9.1	0.40	0.4	3.66

Table 3 (*continued*)

Soil profile, age	Horizon	Depth, cm	Clay, %	Clay B/ clay A	Humus, %	pH	CaCO₃	Exchangeable cations (mg–eq/100 g)		
								Ca	Mg	Na
Kalmykia										
D 530P, 3960±40 BP	A1	53–60	16	0.9	0.62	8.9	5.5	0.18	0.08	3.48
	B1	60–75	15		0.41	8.8	5.3	1.10	7.78	6.52
	C	195–270	14			8.6	6.9	3.68	3.45	11.52
B-3, 4120±70 BP	A	76–84	11	2.2	0.29	8.2	0.10	1.83	3.55	6.96
	B	84–99	26		0.39	8.2	0.20	1.05	2.00	9.13
	C	148–256	16			8.2	8.2	10.40	40.5	8.50
B-17, 4260±120 BP	A	84–94	7	2.1	0.44	7.9	0.2	2.48	1.73	8.26
	B	94–115	15		0.86	7.9	2.6	0.73	0.70	9.57
	C	208–284	16			8.2	8.3	5.25	1.63	7.61
B-1, 4410±100 BP	A1	174–181	9	2.4	0.44	7.9	0.11	1.35	1.08	6.96
	B1	181–199	22		0.60	7.9	1.6	0.80	0.73	7.61
	C	262–327	15			8.2	9.0	5.45	2.95	7.39
D-529, 5100±100 BP	A1	203–213	11	2.2	0.52	7.4	0.0	0.45	0.22	5.65
	B1	213–237	24		0.21	7.6	0.5	0.50	0.32	6.95
	C	285–380	17			8.5	9.1	0.65	0.42	5.98
Peregruznoe										
E-23, modern soil	A1	0–10	15	1.6	1.58	8.1	0.0	0.37	0.47	0.05
	B1	10–27	25		0.93	8.4	0.0	0.15	0.25	0.11
	C	83–180	25			8.5	3.95	1.15	2.27	4.46
D 518, ∼ 1900 BP	A1	21–28	18	1.8	0.93	8.9	0.95	0.125	0.125	0.743
	B1	28–39	33		0.87	9.2	2.67	0.35	0.325	1.347
	C	120–150	28			8.2	3.71	5.5	2.3	9.782
D-520, ∼ 3800 BP	A1	49–58	24	0.9		8.8	3.23	0.65	0.02	2.93
	B1	58–75	23–			8.5	3.50	10.85	6.25	6.52
	C	115–157	19			8.2	3.29	7.10	8.70	6.96
D523, ∼ 5800 BP	A1	35–45	21	0.9	1.0	9.3	2.55	0.15	0.075	0.695
	B1	45–64	20		0.6	9.6	2.86	0.1	0.075	1.282
	C	145–250	20			8.2	3.08	5.35	4.325	6.739
Avilov										
D-505, modern soil	A1	0–10	15	1.53	2.69	6.8	0.0			
	B1	10–26	23		1.86	7.8	0.0			
	C	82–130	20			8.8	4.6			
D 504, ∼ 700 BP	A1	90–102	14	1.8	1.24	8.6	0.0			
	B1	102–122	26		1.14	7.8	0.0			
	C	176–280	23			8.4	3.52			
D-509, ∼ 1750 BP	A1	26–36	21	1.3	0.23	8.7	2.15			
	B1	36–55	28		1.124	8.4	1.08			
D-526, ∼ 1900 BP	A1	50–61	11	1.8	0.52	8.8	0.78			
	B1	61–85	20		0.72	7.8	0.59			
D-510, ∼ 4000 BP	A1	74–86	22	1.0	0.6	8.2	2.15			
	B1	86–103	23		0.5	8.2	3.43			

and palaeosols is the norm. Clay illuviation to the B horizon is another consistent feature of all the soils and palaeosols, again with some exceptions (e.g. the Peregruznoe palaeosols buried at ∼ 3800 and 5800 yr BP).

3.1. Magnetic data

Table 4 summarises the magnetic data obtained for all the sampled soils and palaeosols. Fig. 3(a–d) shows magnetic susceptibility versus soil depth for the five sets of buried soil profiles. Susceptibility values range from ∼ 10–20 × 10^{-8} m³ kg⁻¹ in all of the C horizons to maxima of ∼ 90 × 10^{-8} m³ kg⁻¹ within the A horizon for two of the Avilov palaeosols (∼ 1900 and 700 yr BP). Susceptibility maxima always occur within the upper 40 cm of the soil profiles, reaching enhancement factors of between × 2 and × 4.5, with rapid decreases below this depth. Magnetic susceptibility represents the

Table 4
Magnetic properties of modern and buried soils

Profile	Age , yr BP	Soil horizon	χ, 10^{-8} m^3 kg^{-1}	χ_{fd}, %	χ_{ARM}, 10^{-8} m^3 kg^{-1}	SIRM, 10^{-5} A m^2 kg^{-1}	HIRM$_{100 \text{ mT af}}$, 10^{-5} A m^2 kg^{-1}
Abganerovo							
D 449	Modern soil	A1	46	10.8	129	333	37
		B1	51	12.5	243	312	42
D 451	Modern soil	A1	46	7.7	238	368	29
		B1	63	8.6	228	309	25
414	~ 600	A1	65	11.7	496	497	46
		B1	62	10.8	398	416	43
D 456	~ 1600	A1	41	11.8	193	276	31
		B1	38	15.3	149	239	21
D 455	~ 1600	A1	40	9.8	224	393	41
		B1	54	12.5	220	261	25
D 464	~ 3800	A1	32	3.6	167	277	30
		B1	39	4.7	169	250	33
D 463	~ 5000	A1	29	4.1	124	207	28
		B1	35	9.4	132	252	35
D 455	pm	C	22	6.94	106	184	22
Malyaevka							
D 482	Modern soil	A1	40	8.3	173	367	44
		B1	43	10.1	183	309	63
D 484	Modern soil	A1	38	6.9	191	303	43
		B1	44	11.3	217	258	30
D 480	~ 600	B1	37	11.8	135	234	24
D485	~ 600	B1	38	11.8	150	237	34
D 476	~ 1700	B1	28	5	104	191	34
D 481	~ 3600	B1	24	12.8	101	191	25
D 486	~ 4500	B1	30	8.7	135	231	37
D 486	pm	C	17	5.71	53	152	26
Peregruznoe							
E-23	Modern soil	A1	34	12.2	198	294	32
		B1	34	8	171	249	38
E-24	~ 600	A1	38	9.5	297	441	46
		B1	38	11	178	251	38
D-545	~ 1850	A1	40	11.4.	288	351	35
		B1	39	11.1	197	252	30
D-543	~ 1900	A1	61	9.2	460	499	42
		B1	55	7	283	348	35
D-520	~ 3800	A1	30	9.1	170	256	28
		B1	25	8	138	219	29
D-569	~ 4500	A1	33	9.1	172	242	28
		B1	32	7.7	166	252	31
D-523	~ 5800	A1	36	11.4	218	285	29
		B1	36	6	215	285	29
D-523	PM	C	11	0	55	113	15
Kalmykia							
D-531	Modern soil	A1	51	9.1	283	348	40
		B1	53	8.3	242	330	39
A01-4	~ 600	A1	63	10.2	327	405	28
		B1	55	7.7	265	340	27
D-530	3960±40	A1	33	8.1	166	290	32
		B1	29	6.3	139	260	35
B-3	4120±70	B1	37	8.9	185	260	29
B-17	4260±120	B1	40	7.3	190	292	28
B-1	4410±100	B1	45	6.8	234	342	38

Table 4 (continued)

Profile	Age, yr BP	Soil horizon	χ, 10^{-8} m^3 kg^{-1}	χ_{fd}, %	χ_{ARM}, 10^{-8} m^3 kg^{-1}	SIRM, 10^{-5} A m^2 kg^{-1}	HIRM$_{100\ mT\ af}$, 10^{-5} A m^2 kg^{-1}
Kalmykia							
D-529	5100±50	A1	39	6.2	207	380	40
		B1	44	7.4	218	351	34
D529	PM	C	16	4.8	56	201	40
Avilov							
D-505	Modern soil	A1	59	11.3	389	411	39
		B1	52	9.8	319	365	34
D 504	~ 700	A1	85	11	573	575	35
		B1	76	11.4	452	453	31
D-509	~ 1750	A1	48	12.1	327	372	30
		B1	47	11.9	255	324	30
D-526	~ 1900	A1	84	10.6	460	460	29
		B1	59	10.7	300	327	26
D-510	~ 4000	A1	39	12.1	211	296	26
		B1	33	11.4	191	282	27
D-534	~ 4900	A1	53	11.1	312	407	32
		B1	53	10	287	363	29
D-538	~ 5100	A1	67	11.7	407	476	32
		B1	62	10.9	338	420	31
D-538	PM	C	16	0	71	180	22

total contribution of Fe-bearing minerals in the mineral assemblage and is often controlled by the total ferrimagnetic concentration (Thompson and Oldfield, 1986). The parent material susceptibility values ($\sim 20 \times 10^{-8}$ m^3 kg^{-1}) indicate a magnetite concentration of ~ 0.04%, compared with ~ 0.2% for the most enhanced topsoil. All of the sites have a palaeosol buried at $\sim 600/700$ yr BP. For four of the sites, the susceptibility enhancement is greater in this Middle Ages palaeosol than in the present day soil. The exception, Malyaevka, in the east of the region, shows lower susceptibility values in each of its palaeosols than the present day profiles. At Peregruznoe and Avilov, high susceptibility enhancement is also shown by the palaeosols dated to ~ 1900 yr BP. The oldest palaeosol at Avilov, ~ 5100 yr BP, also shows elevated susceptibility values. Conversely, at all sites, the lowest susceptibility enhancements are associated with the palaeosols dated at between ~ 5000 and 2000 yr BP. For example, at Abganerovo, the lowest topsoil susceptibility value ($\sim 30 \times 10^{-8}$ m^3 kg^{-1}) is associated with the oldest palaeosol, buried ~ 5000 yr BP; at Avilov, Pelegruznoe and Kalmykia, lowest values are displayed by the soils buried at ~ 3800–4000 yr BP. Values of frequency-dependent susceptibility, which reflect the concentration of superparamagnetic (SP), ultrafine-grained ($< \sim 30$ nm in magnetite) grains (Dearing et al., 1996; Maher, 1998), range from 0 to 7% in the parent material but rise to 8–15% in the A and B horizon

samples (Table 4). All the parent material samples display very similar behaviour (Fig. 4) in their acquisition of magnetic remanence (IRM); they are magnetically 'harder' than the overlying A and B horizons. Weakly magnetic minerals, like haematite and goethite, are 'hard', requiring high applied fields to be magnetised. In contrast, strongly magnetic, ferrimagnetic minerals like magnetite and maghemite are magnetically 'soft', acquiring most of their remanence in fields less than 100 milliTesla (mT; e.g. Maher, 1998; Maher et al., 2002). Maximum IRM values for the C horizons are $\sim 150 \times 10^{-5}$ A m^2 kg^{-1}, with ~ 50% of the IRM acquired between 10 and 100 mT and as much as ~ 40% acquired only at high applied fields, from 300 mT to 1 Tesla (T). In contrast, the palaeosol and modern soil A and B horizons display saturation IRM (SIRM) values up to $5\times$ higher (Fig. 4), and acquire up to 10% of their IRM at low applied fields (<10 mT), up to 70% at between 10 and 100 mT, and 15–30% at fields >300 mT. As with the susceptibility data, the IRM values indicate varying ferrimagnetic concentrations in the palaeosols, with peak values most frequently occurring in the Middle Ages (~ 600 yr BP) palaeosols and the modern soils (Table 4). Anhysteretic remanence (ARM, expressed here as the susceptibility of ARM) is particularly sensitive to the presence of sub-micrometre ferrimagnets, ~ 0.03 μm (Özdemir and Banerjee, 1982; Maher, 1998). ARM and magnetic susceptibility show strong direct correlation here, both for the modern and

the palaeosols. Finally, HIRM values show much less direct correlation with susceptibility but are also higher in the modern soils and some of the Middle Ages palaeosols, including those at Peregruznoe, Avilov and Abganerovo. The solonetz profiles (modern and buried) from the sites are characterized by distinctive magnetic profiles, associated with illuvial B horizon formation. These illuvial B horizons are characterized by higher values of susceptibility and frequency dependent susceptibility (%) compared with their A horizons, and lower SIRM and ARM values (Table 4).

3.2. Magnetic extraction

Magnetic extractions were carried out on selected samples from two contrasting sites, Abganerovo and Malyaevka, to identify where the magnetic minerals reside, in terms of clastic grain size (>38 μm and <38 μm), and to identify, by independent means, some of their mineral characteristics (grain size, morphology and composition). In all of the topsoil samples, higher values of susceptibility and ARM are shown by the fine silt fraction, in contrast with the parent material samples,
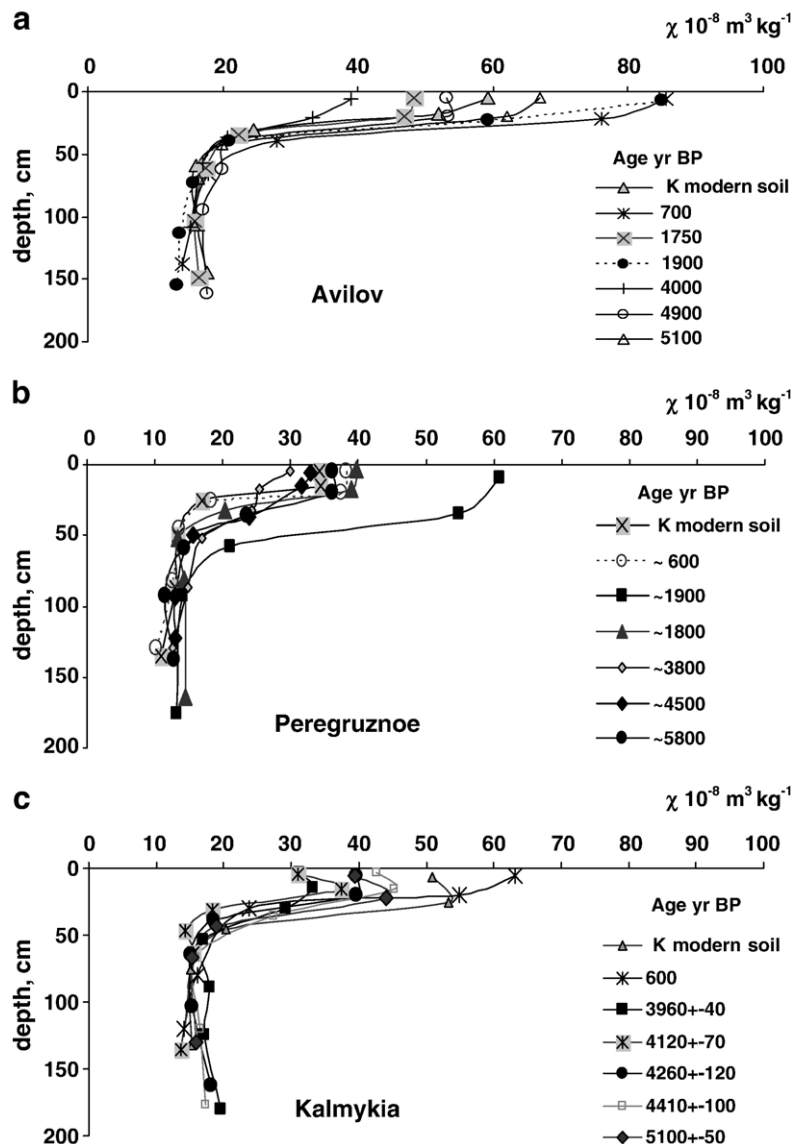
Fig. 3. Magnetic susceptibility with soil depth for modern and palaeosol profiles: a) Avilov; b) Peregruznoe; c) Kalmykia; d) Abganerovo; e) Malyaevka. All profiles in a), b) and c) are kastanozems; for d) and e), K=kastanozem, S=solonetzic soil.
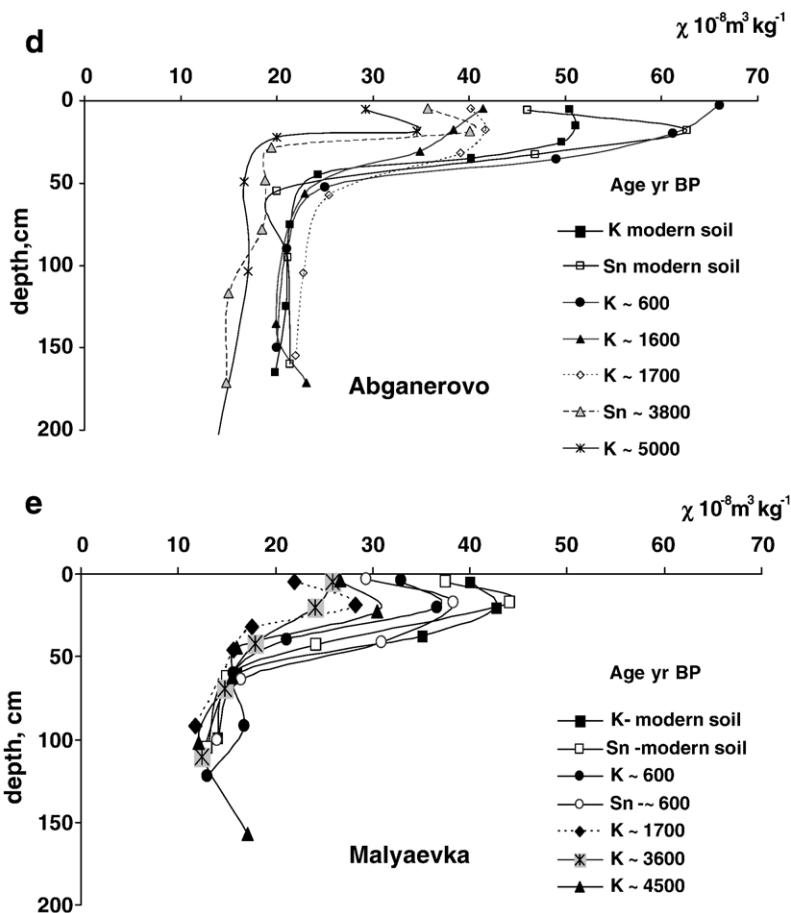
Fig. 3 (*continued*).

in which the coarse clastic fraction is magnetically more dominant. The mean extraction efficiencies, estimated from before- and after-extraction measurements of magnetic parameters, were ∼ 46% of the ARM-carrying grains for the Abganerovo soils (∼ 40% for Malyaevka), and for susceptibility, 43% (Abganerovo) and 34% (Malyaevka). Typical XRD patterns from the magnetic extracts are shown in Fig. 5. The fine-grained (<38 μm) magnetic extracts for the Abganerovo soils contain clay minerals (smectite, chlorite, vermiculite, mica, kaolinite), quartz, feldspars, ferrimagnets (magnetite, maghemite or minerals with composition intermediate between them), and haematite and goethite in different proportions. For Abganerovo, the highest concentrations of ferrimagnets were observed in the ∼ 600 yr BP palaeosol, and for Malyaevka, in the modern soil. The most crystalline ferrimagnets are seen in the parent material samples. All samples contain haematite, with a maximum for the B horizon sample from the ∼ 3800 yr BP palaeosol from Abganerovo. Goethite is less

common than either the ferrimagnets or haematite in these extracts. The fine silt-sized extracts from Malyaevka also contain clay minerals, quartz and feldspars, and ferrimagnets, but display less haematite and almost no goethite. The Malyaevka samples also contain Mg-carbonate (dolomite). Dolomite is characterized by lower solubility than calcite (its presence might account for the reduced efficiency of magnetic extraction for this sample set, as carbonate favours the coagulation of suspension even in the presence of Na-hexametaphosphate as a deflocculant).

The XRD spectra for the coarse-fraction (>38 μm) magnetic extracts identify the dominant presence for the Abganerovo and Malyaevka buried soils of detrital ilmenite, quartz and feldspars (ilmenite is less significant for the modern soil). All the coarse-fraction samples contain highly crystalline magnetite, maghemite and haematite.

Room temperature Mossbauer spectra for the <38 μm magnetic extracts from Abganerovo and Malyaevka

(B horizon samples) reflect superimposed sextets and doublets and independently confirm the presence of magnetically ordered phases. For spectral analysis, the computer model used included two sextets from magnetite, sextets from maghemite and haematite and two doublets for paramagnetic Fe^{3+}. The fine-fraction magnetic extracts ($<38\,\mu m$) were found to contain magnetite/maghemite and haematite (goethite is not identifiable using room temperature Mossbauer analysis).

Transmission electron microscopy of the ultrafine ($<\sim 2\,\mu m$) magnetic extracts showed that they are dominated by two types of opaque crystalline grains of different shape, size and crystallinity (Fig. 6a–c) They also often contain partly transparent clay material. Energy-dispersive X-ray analysis (EDXA) data identifies the principal difference between the opaque particles. As well as Fe, the larger grains ($>1\,\mu m$,

inferred to be of detrital origin) frequently contain Ti and Cr; in contrast, the fine opaque particles ($<0.1\,\mu m$) are enriched in Fe, always Ti-free and often contain Mn (Fig. 6d). Estimations of grain size distributions from electron micrographs show that, compared to their parent materials, the soil horizons are enriched in sub-micrometre magnetic grains. For example, as shown in Fig. 6(a–c), the $<2\,\mu m$ magnetic extracts from profile D-414, Abganerovo (buried at ~ 600 yr BP) are enriched in ultrafine (sub-micrometre) opaque aggregates, clusters and some individual grains of predominantly irregular shape. Some (rare) particles (Fig. 6a) resemble the remnants of magnetite chains of intracellular bacterial origin (e.g. Petersen et al., 1986; Fassbinder et al., 1990) but none display the unique crystal morphologies (e.g. teardrop or bullet shapes) described for intracellular bacterial ferrimagnets.
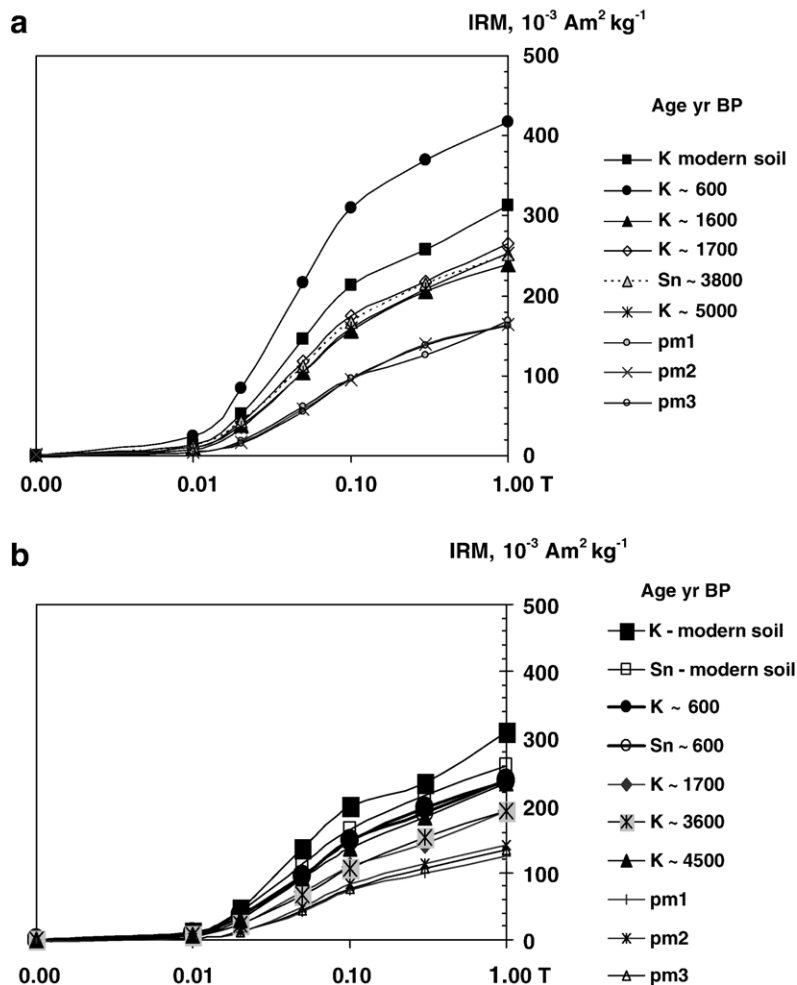
Fig. 4. IRM acquisition for soil profiles from: a) Abganerovo b) Malyaevka; c) Avilov; d) Kalmykia.
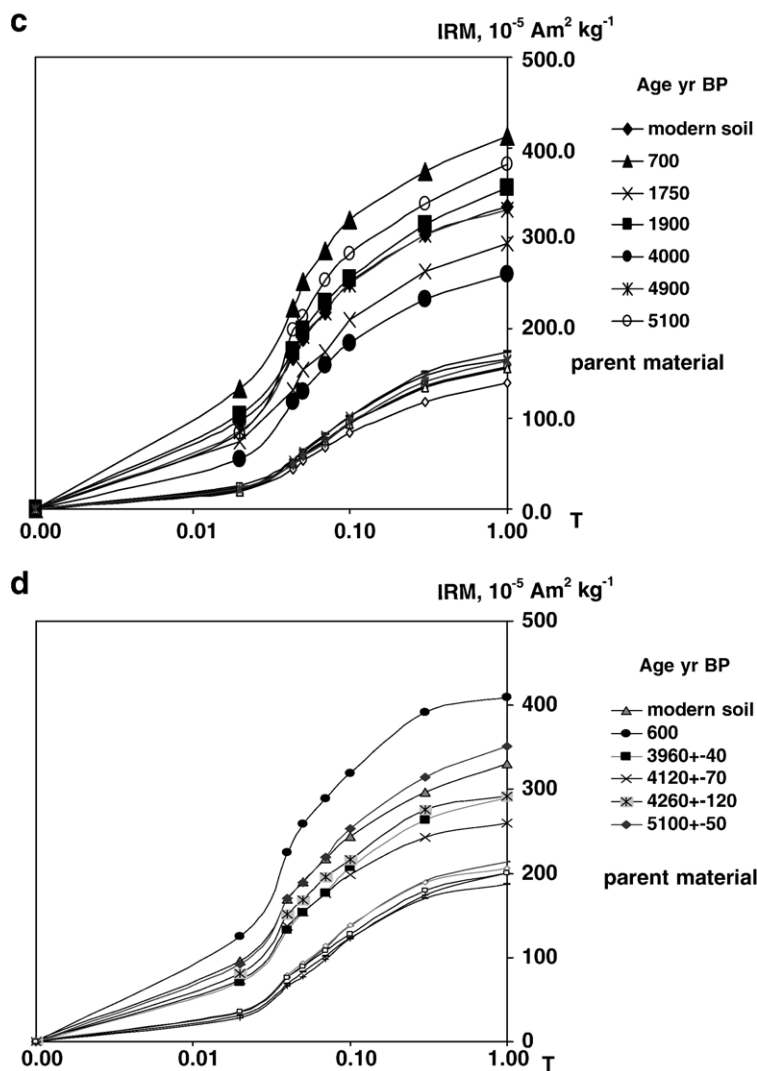
Fig. 4 (*continued*).

Optical microscopy of polished sections of the coarse-fraction (>38 μm) extracts revealed a mixture of opaque (predominant) and transparent grains. Amongst the opaques, reflected light enabled identification of the presence of magnetite, ilmenite, and haematite, with widespread alteration of these detrital grains, from magnetite to martite and ilmenite to haematite. For both soil sets, many of the transparent grains contain inclusions of ferrimagnetic minerals (accounting for their extraction during the magnetic concentration process).

4. Clay mineralogy

The clay fractions of the silty clay loam deposits from which most of the palaeosols have developed are dominated by smectite (35–65%), a mixture of high charge montmorillonite with beidellite (Tables 5 and 6). They also contain mica (17–45%), chlorite, kaolinite, vermiculite, quartz and feldspars. The modern day light kastanozem soils contain in their clay fractions lower smectite contents (up to 15–20%) and the transformation product of smectite — interstratified mica-smectite. Chlorite is absent within the upper 20–30 cm of the modern profiles. We used a pedogenesis intensity (PI) parameter (mica content * 10/smectite content, Alekxeyev, 1999), to estimate the degree of pedogenic clay transformation. For the modern light kastanozems, the PI values increase to ∼ 30–40, in contrast with the parent material, with values of 3–12. The clay mineralogy of the two sets of palaeosols shows that the Abganerovo Middle Ages palaeosol (∼ 600 yr BP)
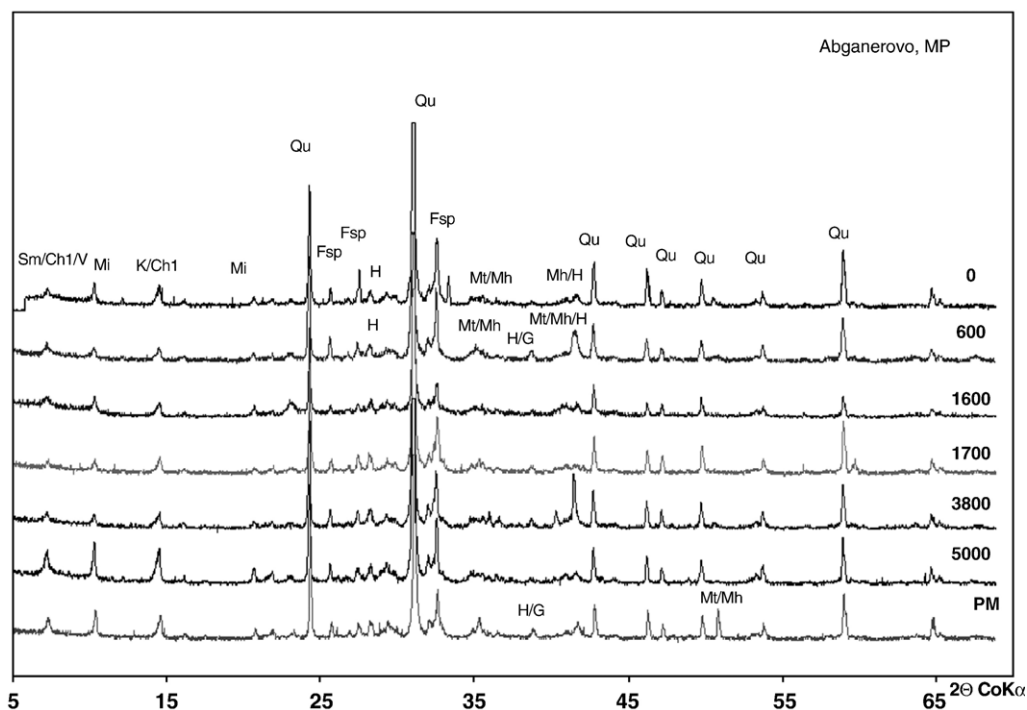
Fig. 5. XRD spectra for <38 μm magnetic extracts from the parent material and B horizon samples from Abganerovo (H – haematite, Mt – magnetite, Mh – maghemite, Qu – quartz, Fsp – feldspars, Sm – smectite, Mi – mica, Chl – chlorite, K – kaolinite).

displays the more differentiated profile, with PI values of ∼ 50–80. In its A horizon, the clay fraction is smectite-poor, rich in residual, fine-grained quartz, and chlorite is absent. However, the A horizon retains a significant clay fraction content and has an unusually high specific surface area value (45 m²/g); such values were observed for soils with similar granulometry but at least 4× higher smectite content (Tables 5 and 6). This palaeosol thus appears to retain some residually solonetzic features. In comparison, the older kastanozem palaeosols from Abganerovo (e.g. ∼ 5000 yr BP and ∼ 1600 yr BP) are characterized by relatively weak profile differentiation. Their clay fractions have a composition rather close to that of the parent material (i.e., rich in smectite and with chlorite present in the upper horizons), and their PI values are ∼ 10 (Table 5), comparable with the parent material. At Malyaevka, all the buried light kastanozems (∼ 4500 yr BP, ∼ 3600 yr BP, ∼ 1700 yr BP and ∼ 600 yr BP) are characterized by weak smectite profile differentiation. It is notable that several of their B horizons contain more weathered material (i.e. with less smectite and larger PI values, 20–45) than the A horizons (PI values of 13–27). The latter may therefore incorporate some parent material admixed during construction of the kurgan. The clay fractions from the A horizons of the buried soils also often con-

tain calcium carbonate (not observed in the B horizons), probably translocated by leaching from the overlying kurgan.

The solonetz profiles of both sites (modern and buried) are characterized by visible clay redistribution and formation of illuvial B horizons, with high clay content and the presence of smectite, with large specific surface area values (Tables 5 and 6). As a result, the A horizons of the buried and modern solonetzes are almost smectite-free. Smectite illuviation results in residual enrichment of the eluvial A horizons in fine quartz and feldspars. PI values for the A horizons vary from ∼ 40 for the palaeosols buried at ∼ 3800 BP to 80–110 for the modern solonetzes. The two oldest solonetzes from the Abganerovo site (∼ 3800 yr BP and ∼ 1600 yr BP) contain chlorite in their upper horizon, indicating weak weathering (given the low stability of chlorite under pedogenesis). In contrast, the upper 30 cm of both modern solonetzes are chlorite-free, suggesting intensified weathering under modern climatic conditions.

4.1. Precipitation estimates

Based on the magnetic properties of all the soils and palaeosols at our five sites, and the mineralogical properties of selected samples from the two representative sites
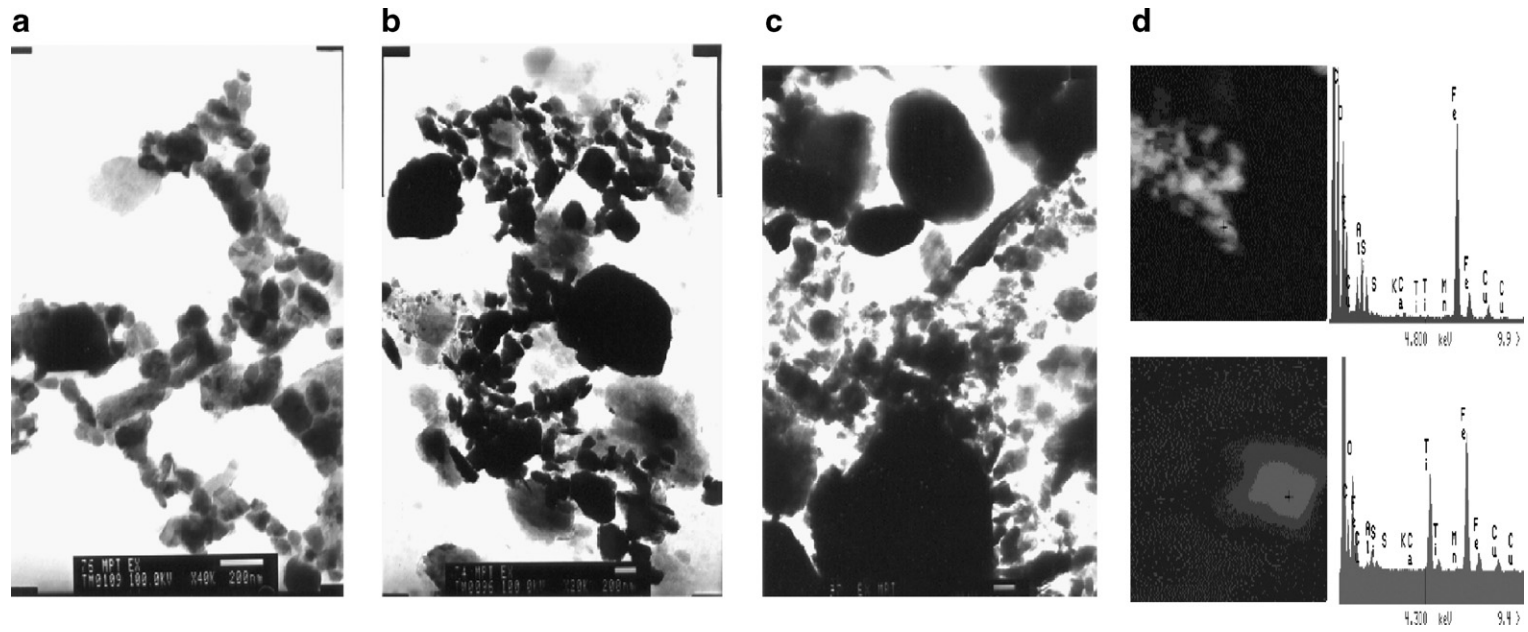
Fig. 6. Transmission electron micrographs for the <38 μm magnetic extracts from B horizon samples, Abganerovo: a) palaeosol buried ∼ 3800 yr BP; b) buried ∼ 5000 yr BP, c) buried ∼ 600 yr BP; d) EDXA data for >1 and <1 μm particles.

Table 5
Clay mineralogy of modern and buried soils from the Abganerovo site

Soil profile, age	Horizon	Depth, cm	k+ chlor.	Mica	Smectite	PI
Light kastanozem						
A99-5, modern	A1	0–10	13	65	23	29
	B1	10–20	21	57	21	27
	B1	20–40	16	53	32	17
	C	105–200	26	31	44	7
D-414,	A1	47–57	18	73	9	81
~ 600 yr BP	B1	57–72	19	67	14	48
	B2	72–87	26	39	35	11
	Bcca	87–102	20	39	41	9
D-456,	A1	90–99	20	40	40	10
~ 1600 yr BP	B1	99–116	19	38	43	9
D-463,	A1	104–114	27	36	37	10
~ 5000 yr BP	B1	114–131	23	46	31	15
	C	250–400	21	28	51	5
Solonetzes						
D-451, modern	A1	0–11	25	67	8	84
	B1	11–25	18	36	46	8
	Cg	120–200	18	36	47	8
D-455,	A1	111–119	30	59	11	53
~ 1600 yr BP	B1	119–134	21	32	47	7
	C	351–371	13	27	60	4
	C	371–431	18	45	36	13
D-464,	A1	79–88	17	67	16	42
~ 3800 yr BP	B1	88–103	19	50	31	16

the topsoil horizons, as also previously found for a more extensive transect of modern soils across the steppe (Maher et al., 2002). It may thus be possible to derive quantitative estimates of climate, specifically annual precipitation, from the palaeosol magnetic properties via the soil magnetism climofunction established for this region. This approach assumes that the *in situ*, pedogenic magnetic susceptibility (i.e. A or B horizon susceptibility minus the parent material susceptibility) is a soil property that develops rapidly (i.e. within decades to centuries) so that it reaches equilibrium with the ambient climate, in line with other upper horizon properties such as pH, humus content and soluble salts (e.g. Crocker and Major, 1955; Hallberg et al., 1978). Conversely, Singer (1992) suggests that time (i.e. the soil-forming duration) is the most important factor for both absolute susceptibility magnitude and susceptibility enhancement for soil chronosequences up to one million years in timespan. It is possible that the buried soils at our five steppe sites may represent both a 'climosequence' and a 'chronosequence'. In terms of a chronosequence, those soils buried at increasingly later timesteps have had incrementally longer periods of soil formation compared with those buried at earlier

(Abganerovo and Malyaevka), some inferences may be drawn regarding possible climatic and environmental changes in this steppe region over the last ~ 5000 years. Given evidence for some incorporation of the overlying kurgan material into the A horizons of the Malyaevka palaeosols, the B horizon soil properties may more reliably reflect the soil-forming environment at the time of soil burial. For our two selected sites, the soil analytical and clay mineralogy data show that for Abganerovo, up until ~ 600 yr BP, light kastanozem soils predominated, characterized by relatively weakly differentiated profiles with weak intensity of mineral weathering. Conversely, at both ~ 600 yr BP and the present day, the soils display increased PI values, with destruction of chlorites, indicating intensification of pedogenesis at these times. At both Abganerovo and Malyaevka, the modern day solonetzes are characterized by increased clay profile differentiation, leaching of exchangeable Na and development towards Mg–solonetz profiles. Similarly, the light kastanozem (but residually solonetzic) soil from Abganerovo, buried at ~ 600 yr BP, also displays evidence of intensified pedogenesis.

The magnetic data obtained for all the soils and palaeosols from each of the five sites show that variable concentrations of magnetite/maghemite have formed in

Table 6
Clay mineralogy of modern and buried soils from the Malyaevka site

Soil profile, age	Horizon	Depth, cm	k+ chlor.	Mica	Smectite	PI
Light kastanozems						
D 482, modern	A1	0–10	29	57	14	40
	B1	10–30	24	59	18	33
	B2	30–43	24	38	38	10
D 480,	A1	23–31	22	44	33	13
~ 600 yr BP	B1	31–55	18	64	18	35
	B2	55–71	32	22	46	5
	C	135–155	27	18	56	3
D 476,	A1	22–31	23	46	31	15
~ 1700 yr BP	B1	31–50	25	50	25	20
	C	78–150	17	17	65	3
D 481,	A1	45–54	33	48	19	25
~ 3600 yr BP	B1	54–77	37	42	21	20
D 486,	A1	68–76	31	50	19	27
~ 4500 yr BP	B1	76–105	24	61	15	40
	C	200–250	23	27	50	5
Solonetzes						
D 484, modern	A1	0–9	15	78	7	107
	B1	9–35	16	57	27	22
	B2	35–50	26	35	39	9
D 485,	A1	43–48	44	44	11	40
~ 600 yr BP	B1	48–73	19	37	44	8
	B2	73–95	39	39	23	17
D 485	C	95–150	22	30	48	6

timesteps. Those soil properties which develop slowly, i.e. over thousands of years (such as some type of weathering index, quartz grain size and shape etc.) may record the impact of time upon these Holocene sequences. However, the sequences may primarily be seen as a 'climosequence'. They have been exposed to different climates through the last ∼ 5000 years, climatic differences which can be expected to be recorded by those rapidly evolving soil properties, including pH, soluble salts, and, arguably, pedogenic magnetic susceptibility. Time-dependence, rather than climate-dependence, of magnetic susceptibility might be envisaged given the requirement for Fe release from primary minerals, for subsequent formation of secondary Fe oxides and oxyhydroxides. However, and as shown here (e.g. Fig. 7a and b), pedogenic magnetic susceptibility appears rarely correlated with total Fe, because it most often reflects the concentration of *trace* amounts of ultrafine-grained magnetite and/or maghemite. In contrast, the weakly magnetic iron oxides,

haematite and goethite, occur at much higher concentrations, accounting for most of the secondary iron oxide component in oxidised soils. The magnetic and mineralogical data for both the modern soil and palaeosol profiles here show that soil formation in the steppe zone produces dispersed ferrimagnetic minerals (magnetite/maghemite) with particle sizes predominantly ≪ 0.1 μm, characterized particularly by high values of magnetic susceptibility and ARM (Fig. 8a–e). The varied shapes and sizes of these ferrite particles indicate predominantly extra- rather than intracellular formation. Laboratory experiments indicate that 'inorganic' magnetite formation is both fast (i.e. within hours) and optimised at near-neutral pH conditions, under initially anoxic conditions, in the presence of mixed Fe^{2+} and Fe^{3+} ions (Taylor et al., 1987). The Fe^{2+} ions may be supplied at least in part via bacterial reduction of Fe under oxygen-poor conditions within the soil microenvironment (Zavarzina et al., 2003). More frequent wetting and drying of the soil can be expected to
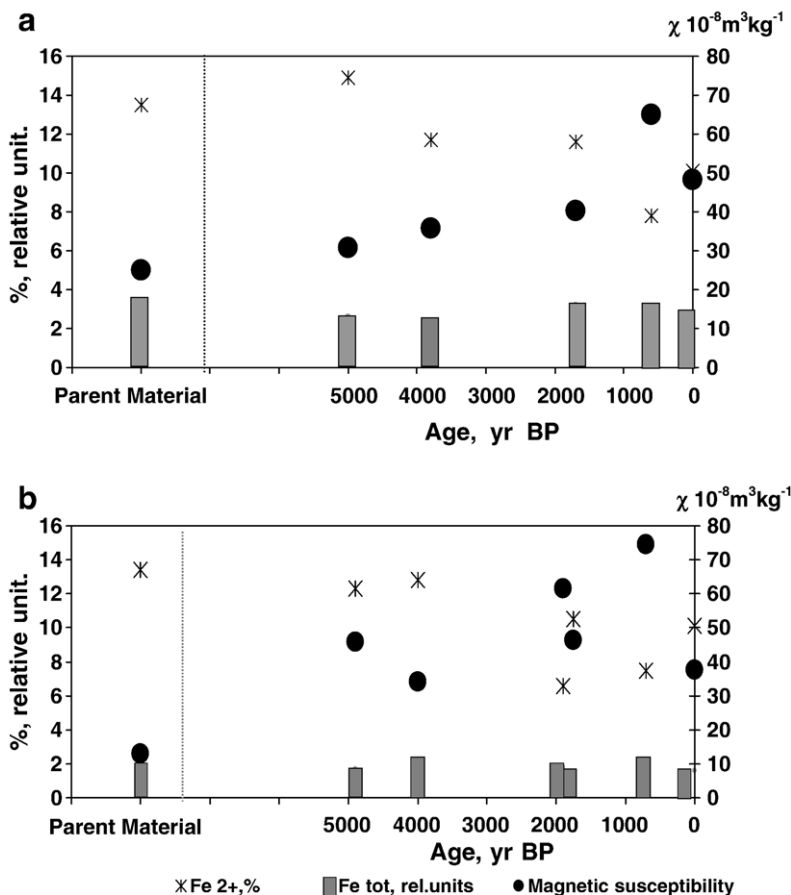

Fig. 7. Magnetic susceptibility, Fe_{bulk} and Fe^{2+} content in silicates for the soils and palaeosols from a) Abganerovo and b) Avilov.
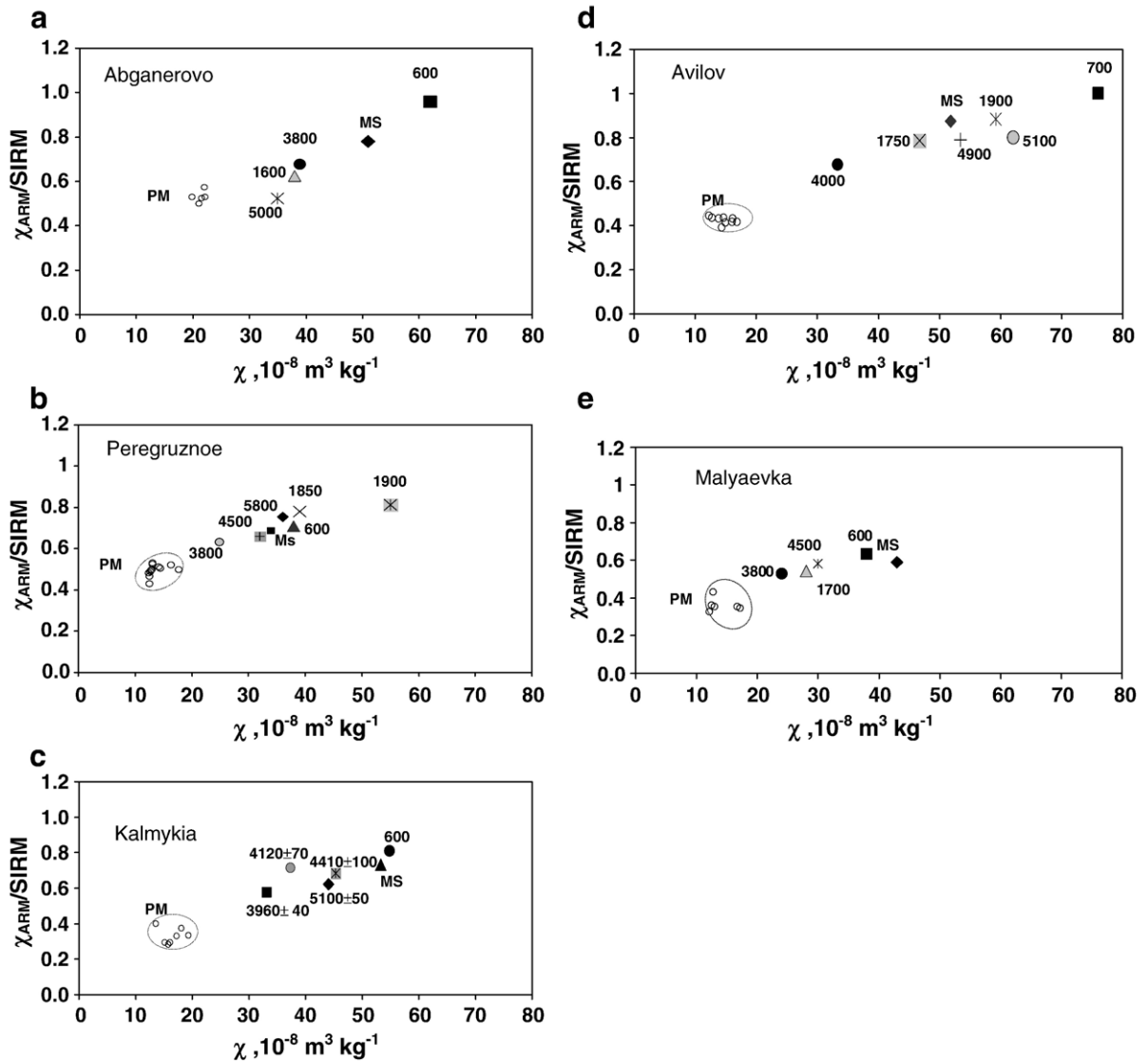
Fig. 8. Biplots of magnetic susceptibility versus χ_{ARM} (normalized by SIRM, to isolate the effect of magnetic grain size dependence, rather than concentration) for each palaeosol timestep for each of the five sites, a) Abganerovo; b) Peregruznoe; c) Kalmykia; d) Avilov; e) Malyaevka. The increasing contribution of fine ferrimagnetic grains (~ 0.03 μm) is indicated by increasing values of χ_{ARM}/SIRM, with overall sample magnetic concentration increasing with increased values of magnetic susceptibility.

produce increasing amounts of pedogenic magnetite; drier, more oxidising conditions leading to increasing proportions of the Fe^{3+}-oxides, goethite and haematite (Maher, 1998). A very minor contribution to the soil magnetic assemblage may derive from intracellular magnetite formation by magnetotactic bacteria, which are also favoured by the existence of micro-anaerobic conditions (Fassbinder et al., 1990). For some of the sites examined here, age control for the palaeosols (from radiocarbon dating) is sufficiently resolved to indicate rapid rates of change of the soil magnetic mineralogy in

response to changing climatic conditions. For example, the Kalmykia site provides five individual timesteps spanning 5100 ± 50 yr BP, 4410 ± 100 yr BP, 4260 ± 120 yr BP, 4120 ± 70 yr BP and 3960 ± 40 yr BP. Significant changes in the pedogenic magnetic properties of the A and B horizons (Fig. 8c) through these timesteps suggest a ferrimagnetic response time of $<\sim 100$ years with regard to changes in soil-forming climate. Similarly, for Avilov (although the time resolution is less robust), A horizon SIRM values appear to vary over timescales of ~ 100–100s years (Fig. 9). In
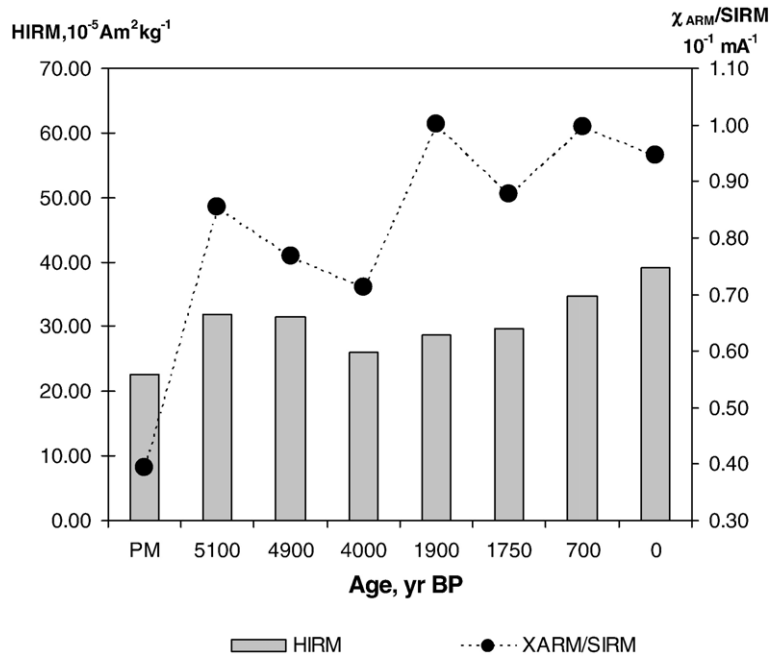
Fig. 9. Changes in χ_{ARM}/SIRM and HIRM through the palaeosol timesteps at Avilov.

contrast, the $HIRM_{100\ mT\ af}$ parameter (reflecting the concentration of haematite/goethite), displays a more muted response, possibly with some apparent gradual overall increase with total soil-forming duration.

Statistical examination of the relationships between the magnetic properties of the modern steppe soils from a transect (Fig. 1) spanning the loess plain from the Caspian Sea to the North Caucasus and major climate variables confirms annual precipitation as the most significant factor (Maher et al., 2002, 2003; Alekseev et al., 2003), with a notably high correlation coefficient ($R^2 = 0.93$):

Annual precipitation (mm) $= 86.4Ln\ (\chi_B - \chi_C) + 90.1$

Alekseev et al. (1988) have previously demonstrated the sensitivity of pedogenic magnetic susceptibility to the conditions of microrelief associated with
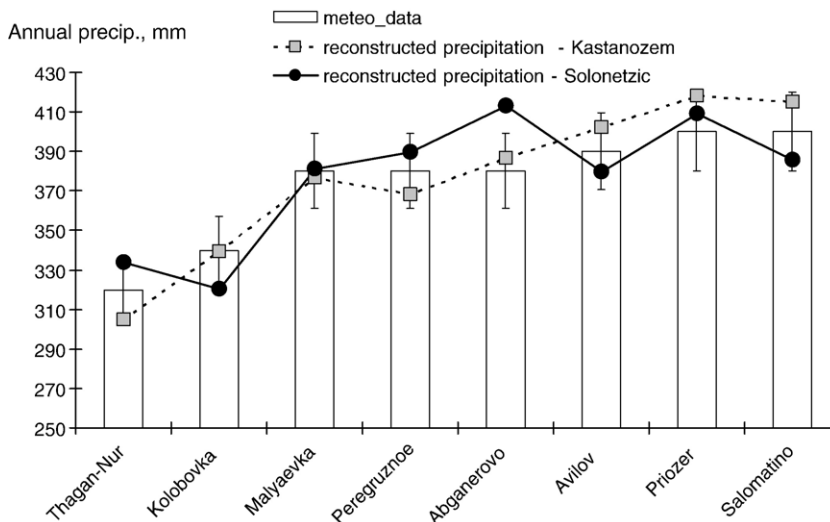
Fig. 10. Testing of soil magnetism climofunction (5% error bar) against modern meteorological data for the two typical modern soil types, kastanozems and solonetzic soils.

the steppe soils. Typically, soil complexes form in the Caspian lowlands, associated with microdepressions of ∼ 15 m in diameter with a relative elevation of about 30 cm. Central parts of the depression are occupied by dark kastanozems, the slopes by light kastanozems, and the peripheral elevations by solonetzes. Differences in susceptibility enhancement for these soils correlate with soil position within this microrelief. Because of their enhanced run-off, the solonetzes receive effectively 10–20 mm 'less' annual precipitation than the lower-lying kastanozem soils (Rode, 1974). To investigate the influence of soil microrelief on the steppe soil magnetism climofunction, we have examined the rainfall/magnetic susceptibility relationship both for kastanozem and solonetz soils. For kastanozems and solonetzic profiles, the climofunction provides rainfall estimates with an accuracy, directly compared with 40-year averaged meteorological data, of ∼ 5% (Fig. 10). However, strongly developed solonetz profiles, with highly developed illuvial horizons (clay B horizon/clay A horizon > 2), provide magnetic susceptibility profile distributions at odds with the climofunction, and are thus excluded from rainfall reconstructions.

Applying the soil magnetism climofunction to our five sets of kurgan-buried palaeosols, we have derived palaeoprecipitation estimates for each of the timesteps represented by the soil sequences (Fig. 11). We can use other, rainfall-indicative, soil property data to test these estimates, especially carbonate and soluble salts concentrations (Fig. 12a and b).

5. Discussion

The data obtained from these suites of palaeosols buried at different times through the last ∼ 5000 years indicate significant changes in rainfall regime over the Russian steppe area over the last ∼ 5000 to 600 years. Climatic desiccation seems to have begun in this region at ∼ 5000 yr BP, reaching minimum precipitation levels at ∼ 3500–4000 yr BP, with up to 15% reduction in annual precipitation compared with the present day. This level of aridization was accompanied by increased soil salinity and enhanced calcification. In contrast, the period from ∼ 2600 to 1600 yr BP appears to have been characterized by alternation of humid and arid conditions. For the Ergeni and Prvolzhskaya Uplands (Peregruznoe and Avilov, respectively), annual precipitation reached a
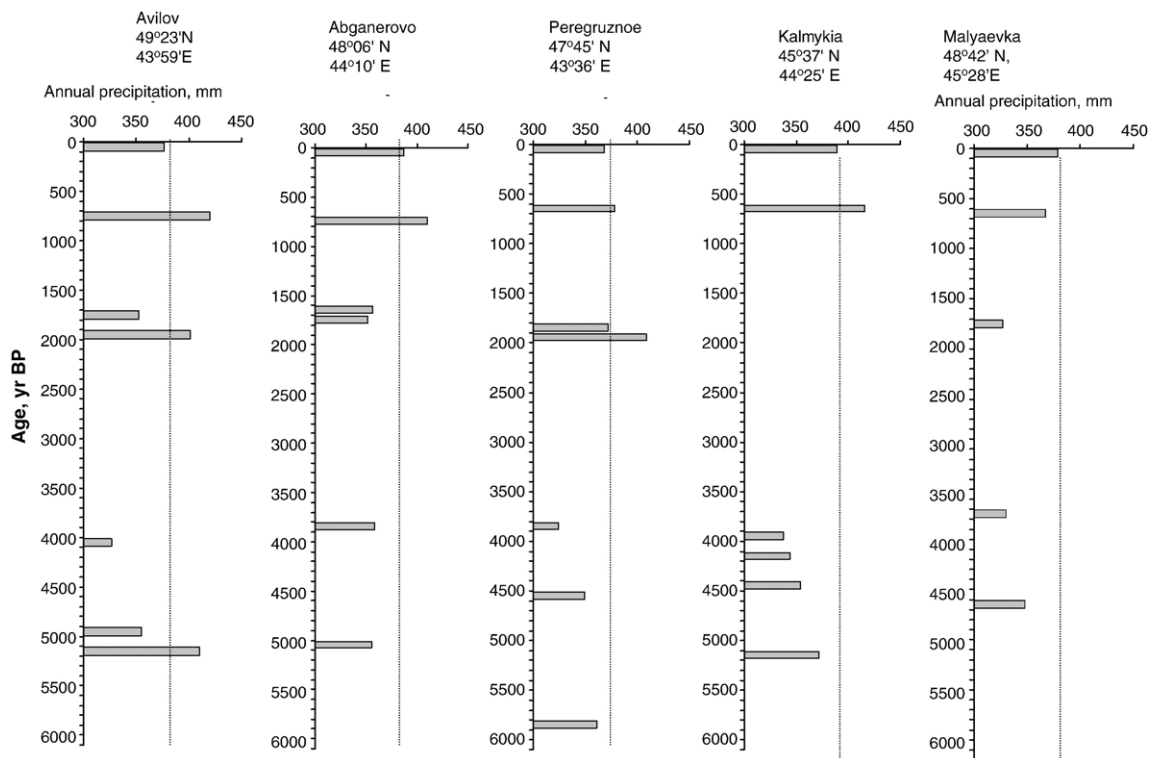

Fig. 11. Rainfall reconstructions for each available palaeosol-derived timestep, from ∼ 5000 yr BP onwards, compared with present day precipitation totals for the five sample sites.
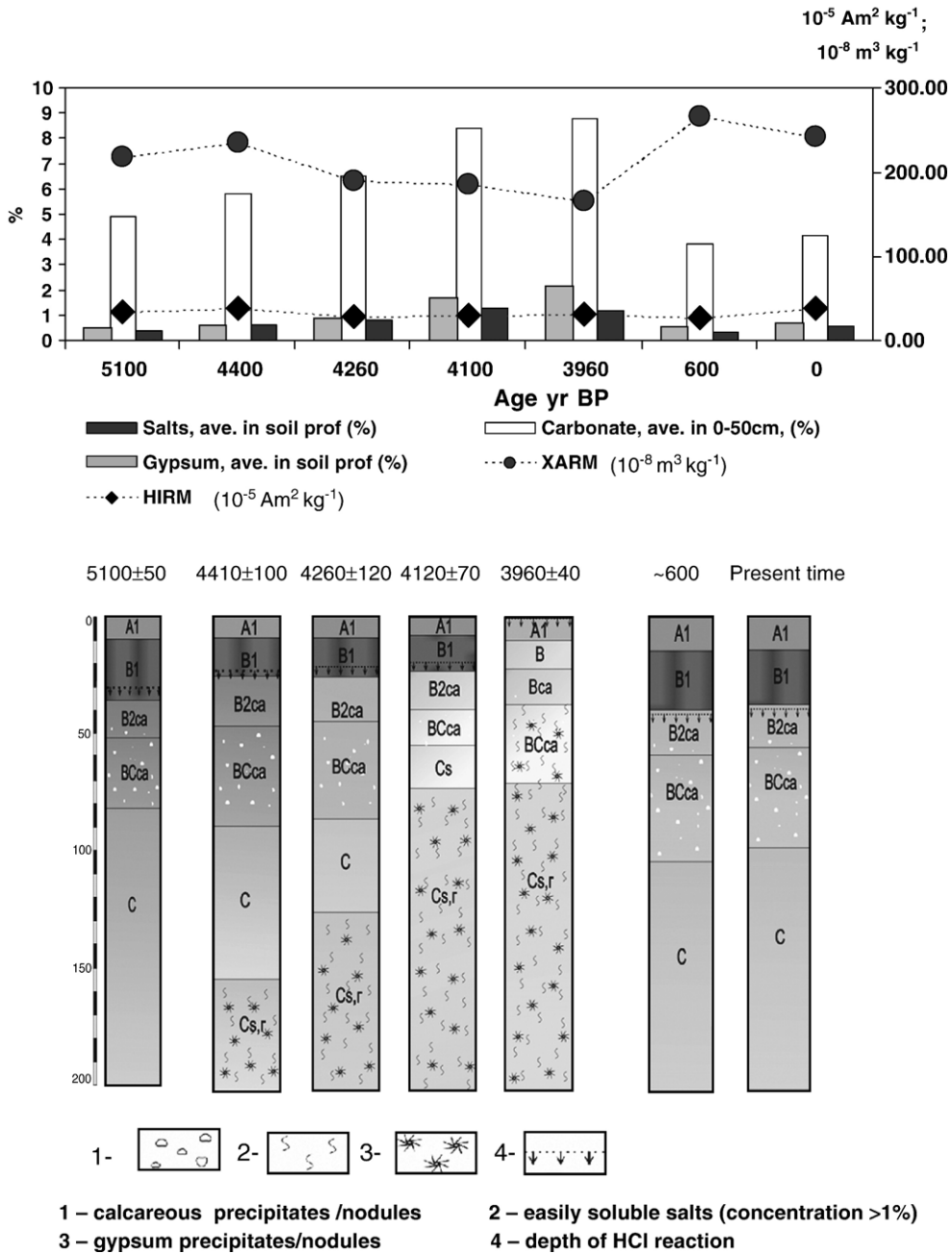
Fig. 12. Magnetic properties, rainfall reconstructions and buried soil properties for the palaeosols and modern soil from the Kalmykia site; a) χ_{ARM}, HIRM and contents of salts, gypsum and carbonate; b) morphological features of the soil profiles.

maximum ($\sim$ +10% compared with the present day) at $\sim$ 1900 yr BP, but subsequently declined by up to $\sim$ 8% at $\sim$ 1700 yr BP. All but one of the Middle Ages ($\sim$ 600 yr BP) palaeosols record another interval of increased annual precipitation, reaching +10% in the Privolzhskaya Upland (Avilov) and between $\sim$ +5 and +8% for the Ergeni Upland (Abganerovo, Kalmykia, Peregruznoe).

For the area of the Caspian lowland to the east (Malyaevka), precipitation levels appear to have been consistently lower than at the other sites, in accordance with the present day rainfall gradient, but with precipitation maxima recorded at the Middle Ages and at the present day. At the present day, due to its degree of continentality and the rainshadow effect of the Caucasus,
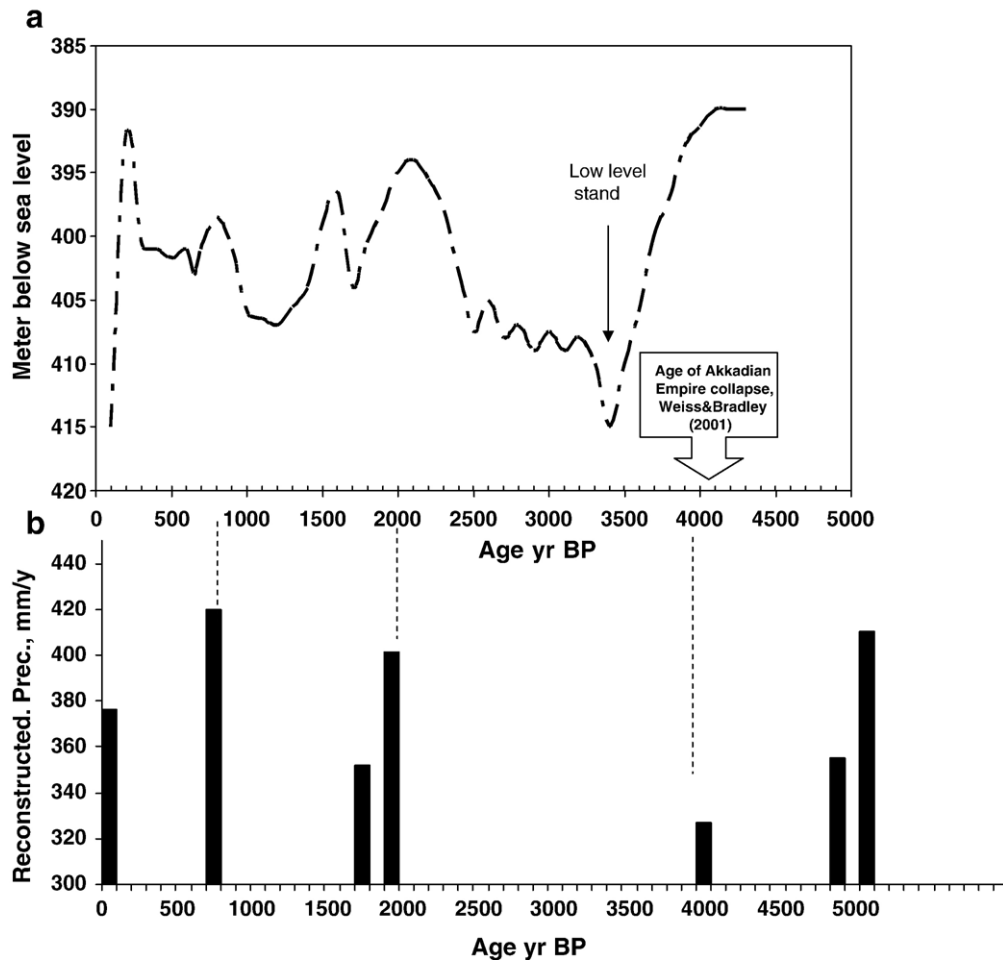
Fig. 13. a) Variations in levels of the Dead Sea from the mid-Holocene (adapted from Enzel et al., 2003); b) reconstructed palaeoprecipitation record from Avilov (this paper).

precipitation in the Russian steppe is low (and variable through the year) and declines towards the east. Mean annual precipitation amounts to ~ 400 mm pa in the west, declining by ~ 50% towards the Caspian lowlands. Our estimates of varying palaeoprecipitation from the mid-Holocene onwards may indicate significant variations in the organization of atmospheric teleconnection patterns, including, for this region, the North Atlantic Oscillation (NAO) and the East Atlantic/Western Russia (EA/WR) dipole system (e.g. Barnston and Livezey, 1987). For example, shifts in the frequency and intensity of storm tracks of the N. Atlantic westerlies – a significant source of precipitation for the steppe region – may have resulted from past changes in the NAO, in turn driven by changes in sea surface temperature and salinity. When in negative mode (i.e. with a reduced pressure gradient between the Azores high and the Icelandic low), N. Atlantic storm tracks are weakened but diverted further south (Chandler

and Jonas, 1999; Cullen et al., 2002). Flow of such southerly storm tracks across the Black Sea and around the south and east of the Caucasus Mountains may have provided enhanced penetration of rainfall into the steppe region at our identified timesteps (~ 1900 and 600 yr BP) in the Holocene. Conversely, the onset of drought conditions at ~ 4000 yr BP might reflect the NAO in dominantly positive mode, resulting in influx of strong, cold and dry winter winds. Some modulation of the NAO signature and influence may also have been incurred by the EA/WR dipole system, characterized by surface pressure anomalies centred over NW Europe and the Caspian region. In positive mode, the EA/WR pattern has high pressure centred on NW Europe and low pressure over the Caspian area, drawing in colder and drier airflow to the steppe region. Warmer and wetter winter conditions arise with the EA/WR in negative mode (Krichak and Alpert, 2005). Initiation of severe and prolonged drought

at ~ 4000 yr BP has been reported for a number of sites around the eastern Mediterranean (e.g. Cullen et al., 2002; Enzel et al., 2003), implicated in collapse of indigenous cultures at this time (Weiss and Bradley, 2001), and linked to atmospheric circulation reorganizations. Whilst acknowledging the discontinuous nature of our palaeoprecipitation data, they appear to show some degree of coherence with, for example, the late Holocene record of palaeolake level data for the Dead Sea (Fig. 13; Enzel et al., 2003). Further palaeoprecipitation data await retrieval from the Russian steppe region as additional kurgans are excavated and their palaeosols revealed and analysed. Magnetic susceptibility measurements are rapid, cheap and easy to make; coupled with the demonstrated robustness of the link with annual precipitation in this region, it appears to provide an effective climate proxy through the Holocene interval.

6. Conclusions

1. Palaeosols buried beneath funeral mounds of different ages on the Russian steppe contain varying concentrations of ultrafine ferrimagnets (magnetite and maghemite) formed *in situ*. X-ray diffraction, Mössbauer spectroscopy and microscopy of magnetic extracts confirm independently that pedogenic formation of magnetite/maghemite in upper soil horizons has occurred to variable extents in the palaeosols and the modern soils.
2. Palaeosols buried within short timesteps of each other (i.e. separated by only ~ 100–100s of years) display significant pedogenic magnetic differences, suggesting that the pedogenic magnetic susceptibility of these soils responded rapidly to changes in ambient climate.
3. Applying a soil magnetism climofunction, calculated from a modern day soil training set, to each set of buried soils enables quantitative estimation of precipitation at each timestep when soil burial occurred. Our palaeoprecipitation estimates identify intervals of reduced precipitation at ~ 5000 yr BP, reaching a minimum at ~ 3500–4000 yr BP, with up to 15% reduction in annual precipitation compared with the present day. In contrast, annual precipitation reached a maximum (~ +10%) at ~ 1900 yr BP, but then declined by up to ~ 8% at ~ 1700 yr BP. All but one of the Middle Ages (~ 600 yr BP) palaeosols record another interval of increased annual precipitation (+5 to +10%). For our easternmost site, precipitation levels have been consistently lower, but with precipitation maxima recorded at the Middle Ages and at the present day.

4. The palaeoprecipitation estimates are in good agreement with other soil properties, especially salt and carbonate content and distribution, which particularly reflect soil hydrological processes, especially in terms of leaching versus evapotranspiration.
5. These new Russian steppe palaeoprecipitation data may correlate with other mid-late Holocene rainfall records from the Middle Eastern region, and reflect at least partly variations in the NAO and EA/WR teleconnection patterns, indicative of significant changes in organization of the atmospheric circulation at intervals from the mid-Holocene onwards.

Acknowledgements

Appendix A. Magnetic measurements

Each sample was dried and packed into 10 cm^3 plastic cylinders. Magnetic susceptibility was measured at low (0.46 kHz) and high (4.6 kHz) frequencies, using a Bartington Instruments MS2 susceptibility meter. ARMs were imparted in an alternating field of 80 mT with a biasing dc field of 0.08 mT (Molspin AF demagnetiser, with dc attachment). The susceptibility of ARM (χ_{ARM}) is calculated by normalizing the ARM by the intensity of the applied bias field. IRMs were imparted in pulsed fields of 10, 20, 50, 100 and 300 mT (Molspin pulse magnetiser) and a dc field of 1000 mT (Newport 4″ Electromagnet). The magnetic hardness of the high-field IRM (HIRM, i.e. acquired beyond 100 mT) was also examined, by first applying a 1 Tesla (T) field to representative samples, to produce an SIRM, which was then af demagnetised in a field of 100 mT. The remanence remaining following this demagnetisation (the $HIRM_{100mT\,af}$) reflects the concentration of stable, high-coercivity minerals, such as haematite (Liu et al., 2002; Maher et al., 2003). HIRMs were AF demagnetised at 100 mT. All magnetic remanences were measured using a fluxgate magnetometer (Molspin Ltd., sensitivity ~ 10^{-7} A m^2).

Appendix B. Independent analyses

For examination of ultrafine (<2 μm) magnetic separates, transmission electron microscopy (JEOL JEM-2000EX), with energy dispersive X-ray analysis (Link Systems Ltd), was used. Mössbauer spectra were

obtained with a MS1101E spectrometer with a constant acceleration drive system (^{57}Co/Cr source with an activity of about 64 mCi). The velocity scale was calibrated relative to Fe and sodium nitroprusside. X-ray diffraction patterns were obtained using CuKα radiation and a DRON-3.0 diffractometer. Samples were stepscanned between 2° and 35° 2θ, using 0.1° 2θ increment with a 5 s counting time per increment. Parallel-oriented specimens were prepared by sedimentation onto 25 mm × 25 mm glass slides of 20 mg aliquots of Mg-, K- and Li-saturated clay. Mg-saturated clays were examined at room temperature, after ethylene glycol solvation and after heating to 300° and 550 °C. K-saturated clays were examined after ethylene glycol solvation and Li-saturated clays — after heating to 250 °C and ethylene glycol solvation. Before saturation with cations, clay fractions from soil horizons were pretreated with 10% H_2O_2 to destroy the organic C.

References

Alekseev, A.O., Kovalevskaya, I.S., Morgun, E.G., Samoylova, E.M., 1988. Magnetic susceptibility of soils in a catena. Pochvovedenie 8, 27–35.

Alekseeva, T.V., Alekseev, A.O., Kovalevskaya, I.S., Osina, G.M., Morgun, Ye.G., 1989. Clay mineralogy of soils on linked sites of Stavropol upland. Soviet Soil Science 21/5, 57–69.

Alekseev, A.O., Alekseeva, T.V., Morgun, E.G., Samoylova, E.M., 1996. Geochemical regularities of iron state in soils of conjugate landscapes of Central Precaucasus. Litologiya i poleznue iskopaemue 1, 12–22.

Alekseev, A.Y.U., Bokovenko, N.A., Boltrik, Y.U., Chugunov, K.A., Cook, G., Dergachev, V.A., Kovaliukh, N., Possnert, G., Van der Plicht, J., Scott, E.M., Sementso, A., Skripkin, V., Vasiliev, S., Zaitseva, G., 2002. Some problems in the study of the chronology of the ancient nomadic cultures in Eurasia (9th–3rd centuries C). Geochronometria 21, 143–150.

Alekseev, A.O., Alekseeva, T.V., Maher, B.A., 2003. Magnetic properties and mineralogy of iron compounds in steppe soils. Eurasian Soil Science 36 (1), 59–70.

Alekxeyev, V.E., 1999. Mineralogy of pedogenesis in steppe and forest-steppe zones of Moldova Kishinev Moldova Inst. of Soil Sci. Agrochemistry and Hydrology, Kishinev, 240 pp. (in Russian).

Alexandrovskiy, A.L., van der Plicht, J., Belinskiy, A.B., Khokhlova, O.S., 2001. Chronology of soil evolution and climatic changes in the dry steppe zone of the Northern Caucasus, Russia, during the 3rd millennium BC. Radiocarbon 43 (2B), 629–635.

Barnston, A.G., Livezey, R.E., 1987. Classification, seasonality and persistence of low frequency atmospheric circulation patterns. Monthly Weather Review 115, 1083–1126.

Borisov, A.V., Alekseev, A.O., Alekseeva, T.V., Demkin, V.A., 2004. Morphological and physicochemical properties of steppe paleosoils as a basis for reconstruction of nature in the past in "Physics, chemistry and biogeochemistry in soil and plant studies". Lublin 34–37.

Biscaye, P.E., 1965. Mineralogy and sedimentation of recent deep-sea clay in the Atlantic Ocean and adjacent seas and oceans. Geological Society of America Bulletin 76, 803.

Chandler, M., Jonas, J., 1999. Atlas of extratropical storm tracks (1961–1998). Tech. Rep. NASA Goddard Institute for Space Studies, New York, NY Available at http://www.giss.nasa.gov/data/stormtracks.

Crocker, R.L., Major, J., 1955. Soil development in relation to vegetation and surface age at Glacier Bay, Alaska. Journal of Ecology 43, 427–448.

Cullen, H.M., Kaplan, A., Arko, R., deMenocal, P.B., 2002. Impact of the North Atlantic Oscillation on Middle Eastern climate and streamflow. Climate Change 55, 315–338.

Dearing, J.A., Dann, R.J.L., Lees, J.A., Loveland, P.J., Maher, B.A., O'Grady, K., 1996. Frequency dependent susceptibility measurements of environmental materials. Geophysical Journal International 124, 228–240.

Demkin, V.A., Ivanov, I.V., 1985. Soil Development in the Caspian Lowland during the Holocene. Russian Academy of Sciences, Pushchino Scientific Centre, 164 pp. (in Russian).

Demkin, V.A., Ryskov, Ya.G., Alekseev, A.O., Gubin, S.V., 1989. Paleopedological study of archaeological monuments of steppe zone. Izvestiya Academy Nauk, Geografichskay Seriya 6, 40–51.

Demkin, V.A., Dergacheva, M.I., Borisov, A.V., Ryskov, Ya.G., Oleynik, S.A., 1998. Soil evolution and climate change in the semidesert zone of Eastern Europe during Late Holocene. Eurasian Soil Science 31 (2), 133–143.

Demkin, V.A., Borisov, A.V., Alekseev, A.O., Demkina, T.S., Alekseeva, T.V., Khomutova, T.E., 2004. Integration of paleopedology and archaeology in studying the evolution of soils, environment, and human society. Eurasian Soil Science 37 (Suppl. 1), 1–13.

Dokuchaev, V.V., 1883. Russian Chernozem St. Peterburg.

Enzel, Y., Bookman, R., Sharon, D., Gvirtzman, H., Dayan, U., Ziv, B., Stein, M., 2003. Late Holocene climates of the Near East deduced from Dead Sea level variations and modern winter rainfall. Quaternary Research 60, 263–273.

Fassbinder, J.W.E., Stanjek, H., Vali, H., 1990. Occurrence of magnetic bacteria in soil. Nature 343, 161–163.

Gelezchikov, B.F., Sergatskov, I.V., Skripkin, A.S., 1995. The Ancient History of Lower Volga Region on the Base of Writing and Archaeological Sources. Volgograd State University Publishing (in Russian).

Gubin, S.V., 1984. Diagenesis of dry steppe soils buried under artificial embankments. Pochvovedenie 6, 5–13 (in Russian).

Hallberg, G.R., Wollenhaupt, N.C., Miller, G.A., 1978. A century of soil development in spoil derived from loess in Iowa. Soil Science Society of America Journal 42, 339–343.

Hounslow, M.W., Maher, B.A., 1996. Quantitative extraction and analysis of carriers of magnetisation in sediments. Geophysical Journal International 124 (1), 57–74.

Hounslow, M.W., Maher, B.A., 1999. Laboratory procedures for quantitative extraction and analysis of magnetic minerals from sediments. In: Walden, J., Oldfield, F., Smith, J.P. (Eds.), Environmental Magnetism: A Practical Guide. Quaternary Research Association, Cambridge, UK, pp. 139–184.

Jenny, H., 1994. Factors of Soil Formation; A system of Quantitative Pedology. Dover Publications, Inc., New York.

Khokhlova, O.S., Kovalevskaya, I.S., Oleynik, S.A., 2001. Records of climatic changes in the carbonate profiles of Russian Chernozems. Catena 43, 203–215.

Khokhlova, O.S., Khokhlov, A.A., Chichagova, O.A., Morgunova, N.L., 2004. Radiocarbon dating of calcareous accumulations in soils of the Holocene chronosequence in the Ural River Valley (Cis–Ural Steppe). Eurasian Soil Science 37, 1024–1038.

Kimball, J.D., Murphy, E.M., Koryakova, L., Yablonksy, L.T. (Eds.), 2000. Kurgans, Ritual Sites, and Settlements: Eurasian Bronze and Iron Age. BAR International Series, vol. 890. Archeopress, Oxford.

Krichak, S.O., Alpert, P., 2005. Decadal trends in the east Atlantic–west Russia and Mediterranean precipitation. International Journal of Climatology 25, 183–192.

Liu, Q.S., Banerjee, S.K., Jackson, M.J., Zhu, R., Pan, Y., 2002. A new method in mineral magnetism for the separation of weak antiferromagnetic signal from a strong ferrimagnetic background. Geophysical Research Letters 29 (6-1-4).

Maher, B.A., 1998. Magnetic properties of modern soils and Quaternary loessic paleosols: paleoclimatic implications. Palaeogeography, Palaeoclimatology, Palaeoecology 137, 25–54.

Maher, B.A., Thompson, R., 1999. Paleomonsoons I: The paleoclimatic record of the Chinese loess and palaeosols. In: Maher, B.A., Thompson, R. (Eds.), Quaternary Climates, Environments and Magnetism. Cambridge University Press, pp. 81–125.

Maher, B.A., Thompson, R., Hounslow, M.W., 1999. Introduction to Quaternary Climates, Environments and Magnetism. In: Maher, B.A., Thompson, R. (Eds.), Quaternary Climates, Environments and Magnetism. Cambridge University Press, pp. 1–48.

Maher, B.A., Alekseev, A., Alekseeva, T., 2002. Variation of soil magnetism across the Russian steppe: its significance for use of soil magnetism as a paleorainfall proxy. Quaternary Science Reviews 21, 1571–1576.

Maher, B.A., Alekseev, A., Alekseeva, T., 2003. Magnetic mineralogy of soils across the Russian steppe: climatic dependence of pedogenic magnetite formation. Palaeogeography, Palaeoclimatology, Palaeoecology 201, 321–341.

Özdemir, Ö., Banerjee, S.K., 1982. A preliminary magnetic study of soil samples from west-central Minnesota. Earth and Planetary Science Letters 59, 393–403.

Petersen, N., von Dobeneck, T., Vali, H., 1986. Fossil bacterial magnetite in deep-sea sediments from the South Atlantic Ocean. Nature 320, 611–615.

Retallack, G.J., 2001. Soils of the Past: an Introduction to Paleopedology, Second Edition. Blackwell, Oxford 600.

Rode, A.A. (Ed.), 1974. Biogeocenosis Bases of Development of Semidesert of Northern PreCaspian. Nauka, Moscow, pp. 3–34.

Schwertmann, U., Taylor, R.M., 1989. Iron oxides, Minerals in Soil Environments, 2nd Edition. SSSA Book Series, vol. 1. Madison, Wisconsin, USA, pp. 379–438.

Shishlina, N.I., Alexandrovsky, A.L., Chichagova, O.A., van der Plicht, J., 2000. Radiocarbon chronology of the Kalmykia Catacomb culture of the west Eurasian steppe. Antiquity 74 (286), 793–799.

Singer, M.J., 1992. Time dependence of magnetic susceptibility of soil chronosequences on the Californian coast. Quat. Res. 37, 323–332.

Skripkin, A.S., 1990. Asiatic Sarmatiya. Saratov State University Publishing (300 pp (in Russian)).

Sergatskov, I.V., 1994. The Sarmatians of Volga–Don steppes and Rome in the first centuries AD. The archaeology of the steppes. Methods and strategies. Napoli 263–277.

Taylor, R.M., Maher, B.A., Self, P.G., 1987. Magnetite in soils: I. The synthesis of single-domain and superparamagnetic magnetite. Clay Minerals 22, 411–422.

Thompson, R., Oldfield, F., 1986. Environmental Magnetism. George Allen and Unwin, London (230 pp).

Weiss, H., Bradley, R.S., 2001. What drives societal collapse? Science 291, 609–610.

Wright, V.P. (Ed.), 1986. Palaeosols: Their Recognition and Interpretation. Blackwell, Oxford. 315pp.

Zavarzina, D.G., Alekseev, A.O., Alekseeva, T.V., 2003. The role of iron-reducing bacteria in the formation of magnetic properties of steppe soils. Eurasian Soil Science 36, 1085–1094.